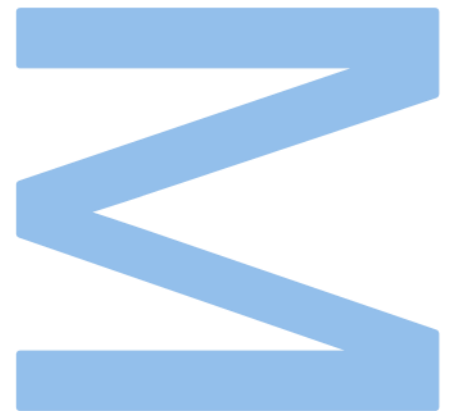


# The role of sigma factors in the formation of bacterial persister cells



**Luisa Lautert Santos**

Master's Degree in Applications in Biotechnology and Synthetic Biology

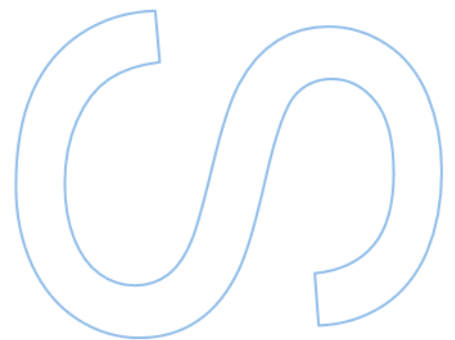
Biology Department and Chemistry and Biochemistry Department  
2022

**Supervisor**

Doctor Yves J. M. Bollen, Assistant Professor, Vrije Universiteit Amsterdam

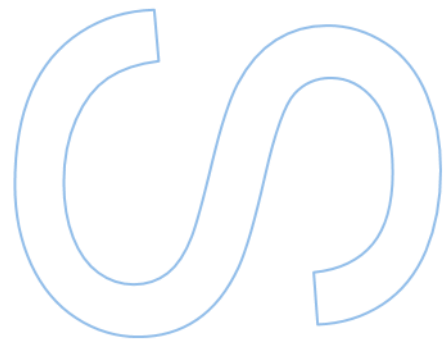
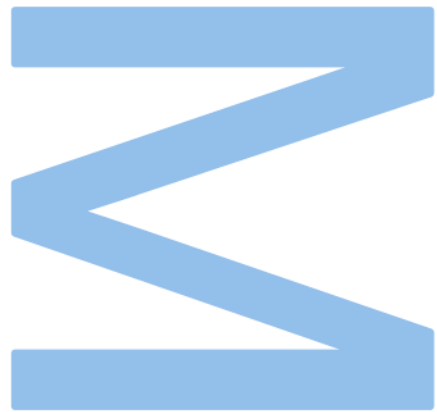
**Co-supervisor**

Doctor Fernando M. dos Santos Tavares, Associate Professor, University of Porto



**U. PORTO**  
**FC** FACULDADE DE CIÊNCIAS  
UNIVERSIDADE DO PORTO

**VU**  **VRIJE  
UNIVERSITEIT  
AMSTERDAM**



*To my beautiful Diana and sweet Theodoro.*

*“Courage is fear that has said its prayers.”*

Dorothy Bernard

# Sworn Statement

I, Luisa Lautert Santos, enrolled in the Master's Degree Applications in Biotechnology and Synthetic Biology at the Faculty of Sciences of the University of Porto hereby declare, in accordance with the provisions of paragraph a) of Article 14 of the Code of Ethical Conduct of the University of Porto, that the content of this dissertation reflects perspectives, research work and my own interpretations at the time of its submission.

By submitting this dissertation, I also declare that it contains the results of my own research work and contributions that have not been previously submitted to this or any other institution.

I further declare that all references to other authors fully comply with the rules of attribution and are referenced in the text by citation and identified in the bibliographic references section. This dissertation does not include any content whose reproduction is protected by copyright laws.

I am aware that the practice of plagiarism and self-plagiarism constitute a form of academic offense.

Luisa Lautert Santos

30-09-2022

# Resumo

De maneira geral, bactérias necessitam se adaptar rapidamente às mudanças do ambiente em que se encontram para que possam sobreviver. A iniciação da transcrição é um ponto crucial da regulação da expressão génica devido à competição de fatores sigma pela RNA polimerase, um mecanismo que permite que as células se adaptem às mudanças no suprimento nutricional, para que possam crescer rapidamente mesmo em ambientes estressantes. As bactérias persistentes podem sobreviver a essas e muitas outras mudanças no ambiente devido à sua alta tolerância a antibióticos e outros tipos de estresse, representando um amplo problema de saúde. O mecanismo de formação de células bacterianas persistentes permanece desconhecido. Neste contexto, este estudo procura compreender melhor a competição entre os fatores sigma e a RNA polimerase, medindo a expressão génica do fator sigma constitutivo ( $\sigma^D$ ) e do fator sigma de resposta geral ao estresse ( $\sigma^S$ ), e investigar se  $\sigma^S$  desempenha um papel na formação de células persistentes. Com este objetivo, genes reporteres foram inseridos no cromossoma de *E. coli* a jusante dos fatores sigma  $\sigma^D$  e  $\sigma^S$ , respectivamente, usando o método de dois plasmídeos da técnica CRISPR-Cas9. Ensaios de crescimento foram realizados com as estirpes mutantes através de citometria de fluxo. Os resultados evidenciaram que em condições favoráveis, tanto  $\sigma^D$  quanto  $\sigma^S$  foram expressos em uma tendência crescente durante as fases exponencial e estacionária de cultivo. Estudos de indução de estresse mostraram uma sobre-expressão de  $\sigma^D$  e uma sub-expressão de  $\sigma^S$  após retirar a fonte de carbono ao meio de cultura. Mais estudos são necessários para esclarecer a hipótese de que  $\sigma^S$  pode fazer parte do mecanismo de formação de células persistentes. Em conclusão, o sistema repórter usado neste trabalho é um valioso contributo para compreender a dinâmica de expressão de cada factor sigma. No futuro será importante perceber mecanismos de regulação pós-transcricionais, para compreender as diferentes dimensões da regulação dos fatores sigma, e consequentemente perceber a sua importância nas adaptações a condições de estresse.

**Palavras-chave:** Competição de fatores sigma, formação de células persistentes, fator sigma constitutivo, fatores sigma alternativos, Crispr-Cas9, sistema repórter de fluorescência.

# Abstract

In general, bacteria need to adapt quickly to changes in the environment in order to survive. Transcription initiation is a crucial point in the regulation of gene expression due to the competition of sigma factors by RNA polymerase, a mechanism that allows cells to adapt to changes in nutritional supply so that they can grow rapidly even in stressful environments. Persister bacteria can survive these and many other changes in the environment due to their high tolerance to antibiotics and other types of stress, representing a wide-ranging health issue. The mechanism of the formation of persister cells remains unknown. In this context, this study seeks to better understand the competition between sigma factors and RNA polymerase, measuring the gene expression of the housekeeping sigma factor ( $\sigma^D$ ) and the general stress response sigma factor ( $\sigma^S$ ), and investigate whether  $\sigma^S$  plays a role in the formation of persistent cells. For this purpose, reporter genes were inserted into the *E. coli* chromosome downstream of the sigma factors  $\sigma^D$  and  $\sigma^S$ , respectively, using the two-plasmid method of the CRISPR-Cas9 technique. Growth assays were performed with the mutant strains by flow cytometry. The results showed that under favourable conditions, both  $\sigma^D$  and  $\sigma^S$  were expressed in an increasing trend during the exponential and stationary phases of cultivation. Stress induction studies showed an over-expression of  $\sigma^D$  and an under-expression of  $\sigma^S$  after removing the carbon source from the culture medium. More studies are needed to clarify the hypothesis that  $\sigma^S$  may be part of the mechanism of persistent cell formation. In conclusion, the reporter system used in this work is a valuable contribution to understanding the expression dynamics of each sigma factor. In the future, it will be important to understand post-transcriptional regulation mechanisms, to understand the different dimensions of the regulation of sigma factors, and consequently to understand its importance in adaptations to stress conditions.

**Keywords:** Sigma factors competition, Persister cells formation, Housekeeping sigma factor, Alternative sigma factors, Crispr-Cas9, Fluorescence reporter system.

# Table of Contents

<b>1. Introduction</b> .....	14
<b>1.1 Sigma factors</b> .....	15
<b>1.2 <i>Escherichia coli</i> sigma factors</b> .....	17
<b>1.3 General trade-off between growth and maintenance</b> .....	18
<b>1.4 The regulator guanosine tetraphosphate</b> .....	19
<b>1.5 Anti-sigma factors</b> .....	20
<b>1.6 Regulation of alternative sigma factors</b> .....	21
<b>1.7 Persister cells</b> .....	22
<b>2. Objectives</b> .....	24
<b>3. Materials and Methods</b> .....	25
<b>3.1 Bacterial strain and growth conditions</b> .....	25
<b>3.2 Plasmids</b> .....	25
<b>3.3 Genome insertion of fluorescent reporters</b> .....	28
<b>3.4 Microscopy imaging</b> .....	30
<b>3.5 Growth experiments</b> .....	30
3.5.1 Sigma factors expression at average population cell level .....	31
3.5.2 Sigma factors expression at single cell level .....	31
3.5.3 Sigma factors expression in stress-inducing conditions .....	32
3.5.4 Data analysis .....	32
<b>4. Results</b> .....	33
<b>4.1 Genome insertion of fluorescent reporters</b> .....	33
<b>4.2 Microscopy imaging</b> .....	34
<b>4.3 Growth experiments</b> .....	35
4.3.1 Sigma factors expression at average population cell level .....	35
4.3.2 Sigma factors expression at single cell level .....	38
4.3.3 Sigma factors expression in stress-inducing conditions .....	42



<b>5. Discussion .....</b>	<b>46</b>
<b>6. Conclusions and future perspectives .....</b>	<b>51</b>
<b>7. References .....</b>	<b>52</b>
<b>8. Supplementary material .....</b>	<b>58</b>

# List of Tables

<b>Table 1 – E. coli sigma factors.....</b>	<b>17</b>
<b>Supplementary Table 1 - List of primers used in this study.....</b>	<b>58</b>
<b>Supplementary Table 2 - Clone 4 DNA sequencing after the reporter insertion .....</b>	<b>59</b>
<b>Supplementary Table 3 - Clone 10 DNA sequencing after the reporters' insertion ....</b>	<b>60</b>

# List of Figures

<b>Figure 1</b> - Schematic representation of core-RNAP binding a sigma factor to form the holoenzyme, adapted from Sutherland (2018) .....	16
<b>Figure 2</b> - Schematic representation of the sigma factor competition during transcription (Österberg, 2011) .....	16
<b>Figure 3</b> - Schematic representation of why persister cells are a health threat (Lewis, 2010) .....	22
<b>Figure 4</b> - Schematic representation of the designed pTargetF plasmids for Crispr-Cas9 two-plasmid system for <b>(A)</b> rpoD gene and <b>(B)</b> rpoS gene .....	26
<b>Figure 5</b> - LB plate from colony PCR .....	27
<b>Figure 6</b> – Schematic gene representation of the fluorescent reporter genes insertions in E. coli genome downstream the housekeeping sigma factor $\sigma^D$ and the stress response sigma factor $\sigma^S$ .....	30
<b>Figure 7</b> - 96-well-filled plate layout for plate reader experiment.....	31
<b>Figure 8</b> – Agarose gel electrophoresis analysis of Colony PCR products from E. coli MG1655 cells after Crispr-Cas9 system experiments.....	33
<b>Figure 9</b> – E. coli MG1655 cells curing from the CRISPR-Cas9 plasmids on LB plates supplemented with antibiotics. ....	34
<b>Figure 10</b> - Fluorescence microscopy images in the red and green channel and grayscale of E. coli MG1655 cells <b>(A)</b> wild-type, <b>(B)</b> strain containing the red reporter after $\sigma^D$ and <b>(C)</b> the strain containing the red and green reporter after $\sigma^D$ and $\sigma^S$ , respectively.....	35
<b>Figure 11</b> – E. coli MG1655 cell growth and autofluorescence from plate reader experiment, used as control .....	36
<b>Figure 12</b> – E. coli MG1655 generated strain containing the single red reporter on $\sigma^D$ cell growth and sigma factors expression from plate reader experiment .....	36
<b>Figure 13</b> – E. coli MG1655 generated strain containing both red and green reporters on $\sigma^D$ and $\sigma^S$ cell growth and sigma factors expression from plate reader experiment .....	37
<b>Figure 14</b> – E. coli MG1655 autofluorescence acquired with flow cytometry, used as control.....	38
<b>Figure 15</b> – E. coli MG1655 autofluorescence density plots, acquired with flow cytometry, used as control .....	39
<b>Figure 16</b> – E. coli MG1655 generated strain containing the red reporter downstream $\sigma^D$ and the green reporter downstream $\sigma^S$ fluorescence signal acquired with flow cytometry .....	39
<b>Figure 17</b> – Sigma factors expression of E. coli MG1655 generated strain containing the red reporter downstream $\sigma^D$ and the green reporter downstream $\sigma^S$ in fluorescence density plots, acquired with flow cytometry .....	40
<b>Figure 18</b> – <b>(A)</b> Average autofluorescence of wild-type and <b>(B)</b> the average sigma factors expression of E. coli MG1655 constructed strain containing the red reporter downstream $\sigma^D$ and the green reporter downstream $\sigma^S$ , acquired with flow cytometry. ....	41
<b>Figure 19</b> – <b>(A)</b> Average sigma factors expression of E. coli MG1655 constructed strain containing the red reporter downstream $\sigma^D$ and the green reporter downstream $\sigma^S$ , acquired with flow cytometry and corrected by wild-type autofluorescence and <b>(B)</b> Cell	

growth of E. coli MG1655 constructed strain containing the red reporter downstream $\sigma^D$ and the green reporter downstream $\sigma^S$ .....	41
<b>Figure 20</b> - E. coli MG1655 generated strain containing the red reporter downstream $\sigma^D$ and the green reporter downstream $\sigma^S$ fluorescence signal acquired with flow cytometry during stress-inducing conditions .....	43
<b>Figure 21</b> - Sigma factors expression of E. coli MG1655 generated strain containing the red reporter downstream $\sigma^D$ and the green reporter downstream $\sigma^S$ in fluorescence density plots, acquired with flow cytometry during stress-inducing conditions .....	44
<b>Figure 22</b> – Average sigma factors expression of E. coli MG1655 constructed strain containing the red reporter downstream $\sigma^D$ and the green reporter downstream $\sigma^S$ , acquired with flow cytometry during stress-inducing conditions.....	44
<b>Figure 23</b> – (A) Average sigma factors expression of E. coli MG1655 constructed strain containing the red reporter downstream $\sigma^D$ and the green reporter downstream $\sigma^S$ , acquired with flow cytometry during stress-inducing conditions and corrected by wild-type autofluorescence. (B) Cell growth of the same strain acquired under stress-inducing conditions .....	45
<b>Supplementary Figure 1</b> – E. coli MG1655 generated strain containing the single red reporter on $\sigma^D$ cell growth and sigma factors expression from plate reader experiment .....	61
<b>Supplementary Figure 2</b> – E. coli MG1655 generated strain containing both red and green reporters on $\sigma^D$ and $\sigma^S$ cell growth and sigma factors expression from plate reader experiment.....	61
<b>Supplementary Figure 3</b> - E. coli MG1655 autofluorescence acquired with flow cytometry, used as control .....	62
<b>Supplementary Figure 4</b> - E. coli MG1655 generated strain containing the red reporter downstream $\sigma^D$ and the green reporter downstream $\sigma^S$ fluorescence signal acquired with flow cytometry.....	64
<b>Supplementary Figure 5</b> - E. coli MG1655 autofluorescence density plots, acquired with flow cytometry, used as control .....	65
<b>Supplementary Figure 6</b> - Sigma factors expression of E. coli MG1655 generated strain containing the red reporter downstream $\sigma^D$ and the green reporter downstream $\sigma^S$ in fluorescence density plots, acquired with flow cytometry .....	67

# List of Abbreviations

<b>RNAP</b>	RNA polymerase enzyme
<b>PSS</b>	Protein-synthesizing system
<b>ppGpp</b>	Guanosine tetraphosphate
<b>pppGpp</b>	Guanosine pentaphosphate
<b>Rsd protein</b>	Regulator of sigma D protein
<b>sRNAs</b>	Small RNAs

# 1. Introduction

Bacteria are constantly exposed to different stressful environments, experiencing temperature or pH variation or more general stresses, such as entry into stationary phase or nutrient depletion (Kim, 2020). Even in the same environment, conditions can change very rapidly and in order to survive, bacteria must adapt. This ability of rapidly adjusting to variations in environmental conditions is essential for the growth and survival of bacteria in their natural environment (Cavaliere et al., 2018). Understanding how bacteria adjust to changes in nutritional supply to grow quickly in various situations is a challenging subject in bacterial physiology (Pavlov, 2013).

For rapid growth during environmental changes, bacterial cells must adapt their enzyme levels to efficiently metabolize different kinds of nutrients in different surroundings (Pavlov, 2013). One point essential for cellular adaptability is the mechanism of directing the RNA polymerase to different sets of genes at the transcription initiation (Sharma, 2010; Li et al., 2019; Oguienko et al., 2021).

The dissociable units responsible for this mechanism are the sigma factors, which bind to core-RNAP and form the holoenzyme (Cho et al., 2014; Davis et al., 2017). They confer promoter selectivity on the RNAP, and through this process, the holoenzyme RNAP dictates what genes will be expressed and when (Feklístov et al., 2014). All bacteria have a housekeeping sigma factor that leads the holoenzyme of RNAP to most genes to be transcribed, as well as alternate sigma factors that direct RNAP to genes involved in adaptive responses (Österberg, 2011). Therefore, the number of alternative sigma factors is directly related to the number of environments the bacterium can adapt to (Sharma, 2010).

In transcription initiation, the sigma factors compete for the limited amount of RNAP inside the cell (Kandavalli, 2016; Davis et al., 2017). When conditions are favourable, the housekeeping sigma  $\sigma^D$  wins the competition, and also during the exponential phase of growth (Baptista et al., 2022). When conditions are not ideal or growth reaches the stationary phase, the sigma factor required for generalised stress response  $\sigma^S$  tends to bind core-RNAP, as well as the other alternative sigma factors (Baptista et al., 2022).

In bacteria, as in every living organism, there is a general trade-off between reproduction and survival; the metabolic resources must be allocated for one or the other (Nystrom 2004). Generally, when conditions are favourable, reproduction is prioritised, and maintenance is preferred when conditions are not. RNA Polymerase is one of these metabolic resources, and its allocation depends on the sigma factor competition.

However, it has been suggested that during favourable conditions, although the big majority of cells are growing fast, a small fraction is slow growing or not growing at all (Kaldalu et al., 2020). And besides most of these cells are stress sensitive, this small fraction is very stress tolerant. Considering the sigma factor competition, the significant fraction of cells probably has more  $\sigma^D$  activated during transcription, and the small population that is stress-tolerant probably has more  $\sigma^S$ .

In this context, we hypothesized that under growth-supporting conditions, a small population of cells is already expressing more  $\sigma^S$ , thus preparing for more stressful conditions. These cells may be better equipped for surviving subsequent difficult conditions. Since these cells are stress-tolerant and slow-growing, they can be persisters cells, which are slow-growing variants of regular cells highly tolerant to antibiotics or other kinds of stress (Lewis, 2010). It has been known that  $\sigma^S$  and the alarmone molecule ppGpp levels are high in persister cells, but the mechanism that causes persistence is not yet established (Radzikowski et al., 2016). On this basis,  $\sigma^S$  is a good candidate for responsible for inducing persisters formation (Radzikowski et al., 2016). For this reason, this study focuses on understanding how important  $\sigma^S$  is to persister cell formation.

## 1.1 Sigma factors

Bacterial RNA polymerase enzyme (RNAP) is responsible for gene expression and crucial to its regulation (Sutherland, 2018; Bačun-Družina et al., 2011). It can be found inside the cell in two forms: the core enzyme, which can bind to non-specific DNA but cannot recognise promoters, and the holoenzyme, which has the affinity for non-specific DNA reduced and is directed to different promoters, so sets of genes with specific function can be transcribed (Sutherland, 2018; Bačun-Družina et al., 2011; Feklístov et al., 2014). The core-RNAP contains five polypeptide subunits, two alpha ( $\alpha$ ), which assemble the enzyme, one beta ( $\beta$ ), which catalyses the synthesis of RNA, one beta' ( $\beta'$ ), which binds to the DNA template and one omega ( $\omega$ ), which restores RNAP to its functional form in vitro (Bačun-Družina et al., 2011; Cho et al., 2014; Sutherland, 2018). The holo-RNAP has all five subunits and a sixth subunit, a sigma factor (Gopalkrishnan, 2014; Kandavalli, 2016; Davis et al., 2017).

The sigma factors are the dissociable subunits of bacterial core-RNAP that, when associated with it, form the holoenzyme, and direct it to the different transcription start sites, so different sets of genes can be transcribed (Österberg, 2011; Sharma, 2010). They are required for transcription to initiate and guide RNAP through promoter

recognition and opening and synthesising of the first few nucleotides (Feklístov et al., 2014; Li et al., 2019).

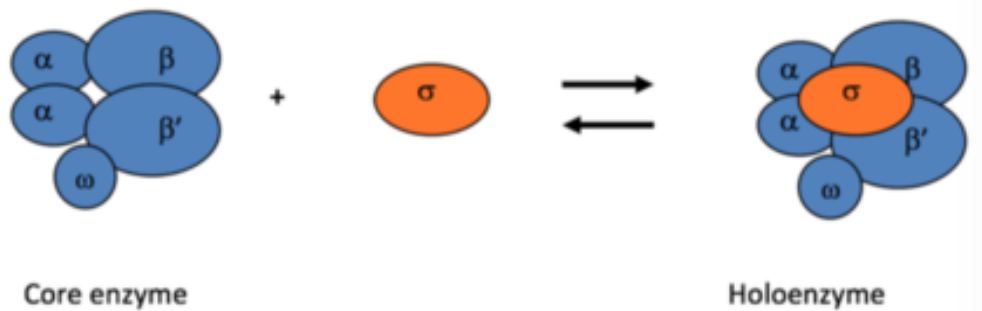


**Figure 1** - Schematic representation of core-RNAP binding a sigma factor to form the holoenzyme, adapted from Sutherland (2018)

The sigma factors are the dissociable subunits of bacterial core-RNAP that, when associated with it, form the holoenzyme, and direct it to the different transcription start sites, so different sets of genes can be transcribed (Österberg, 2011).

Therefore, the sigma factors confer promoter selectivity on the RNAP and through this process, the holoenzyme RNAP dictates what genes will be expressed and when (Österberg, 2011; Feklístov et al., 2014). The direction of RNAP to bind specific promoters is an important point of gene expression regulation, which is essential for cellular adaptability (Sharma, 2010; Baptista et al., 2022). The control of transcription initiation is a primary access point for regulating gene expression in all domains of life, and it is crucial in prokaryotes (Österberg, 2011; Feklístov et al., 2014).

All bacteria contain a housekeeping sigma factor, which directs the holoenzyme of RNAP to most genes to be transcribed, and alternative sigma factors, which direct RNAP to genes related to adaptive responses (except for the *mycoplasma* pathogens) (Österberg, 2011; Chauhan et al., 2016).

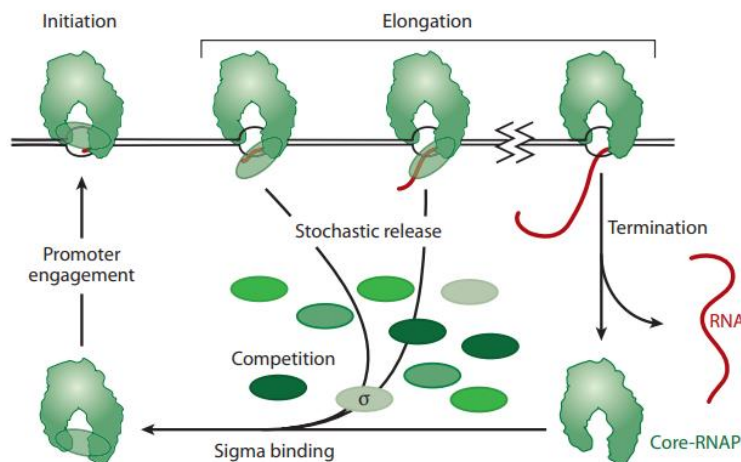


**Figure 2** - Schematic representation of the sigma factor competition during transcription (Österberg, 2011) Each sigma factor competes for the free core-RNAP to form the holoenzyme and then is released during transcription elongation so it can start the competition again (Österberg, 2011).



A large number of sigma factors in bacteria help switch transcription in response to a wider variety of environmental signals, so the number of alternative sigma factors depends on the bacterium’s lifestyle (Sharma, 2010; Österberg, 2011). Each alternative sigma factor promotes the transcription of genes required for coping with stress or responding to environmental and physiological signals (Feklístov et al., 2014). The *Streptomyces coelicolor* bacterium, for example, contains 60 alternative sigma factors (Österberg, 2011) and the *Bacillus subtilis* has 10 different sigma factors (Haldenwang, 1995). The *Mycoplasma genitalium* bacterium is an exception and only possesses a single sigma factor (Österberg, 2011; Feklístov et al., 2014).

The core-RNAP concentration remains relatively constant inside the cell and at a lower amount than the sigma factors, so they have to compete for it (Baptista et al., 2022; Österberg, 2011). Each sigma factor competes for the free core-RNAP to form the holoenzyme and then is released during transcription elongation so it can start the competition again (Österberg, 2011). In addition to intracellular concentration, another feature that influences the competition directly is the high affinity for the housekeeping sigma factor and lower affinity to alternative sigma factors (Sharma, 2010). This difference in affinity is essential for this system to be efficient; accordingly, only a tiny fraction of promoters can recognise more than one sigma factor (Baptista et al., 2022).

## 1.2 *Escherichia coli* sigma factors

As stated previously, a high number of sigma factors are directly related to the capacity of bacteria to adapt to various environments (Sharma, 2010; Cho et al., 2014). *E. coli* has seven different sigma factors, which reflects that this bacterium goes in different environments like the soil, the water, and animals’ guts (Österberg, 2011; Cho et al., 2014). Each one is required to transcribe genes with specific functions so that the cell can adapt to these environments (Nyström, 2004). Besides the housekeeping sigma, at least four of *E. coli*’s sigma factors are required to respond to stress, two are involved in heat shock response, and one is in nitrogen regulation (Farewell, 1998; Shimada, 2021).

**Table 1** – *E. coli* sigma factors. Adapted from Österberg (2011) and Bačun-Družina et al. (2011)

Sigma factor	Gene	Related sets of genes
$\sigma^{70/D}$	<i>rpoD</i>	Most genes (housekeeping sigma factor)
$\sigma^{54/N}$	<i>rpoN</i>	Nitrogen utilisation of alternative carbon sources, assembly of motility organs

$\sigma^{38/S}$	<i>rpoS</i>	General stress response
$\sigma^{32/H}$	<i>rpoH</i>	Heat-shock stress
$\sigma^{28/FliA}$	<i>rpoF</i>	Flagella filament subunits, proteins involved in bacterial taxis
$\sigma^{24/E}$	<i>rpoE</i>	Membrane stress, availability of iron, extreme heat stress
$\sigma^{19/FecI}$	<i>fec</i>	<i>Fec</i> genes for iron transport

The housekeeping sigma factor of *E. coli* is  $\sigma^D$ , also known as  $\sigma^{70}$ , and it directs RNAP to most genes to be transcribed. This sigma factor has the highest affinity for core-RNAP and recognises promoters of growth-related and housekeeping genes, including DNA replication, membrane biosynthesis and ribosome production (Sharma, 2010; Bačun-Družina et al., 2011; Nyström, 2004). Also, most genes of the protein-synthesizing system (PSS) are transcribed in the presence of  $\sigma^D$  (Nyström, 2004). Considering the genes are growth-related, the  $\sigma^D$  usually wins the competition during the exponential phase (Baptista et al., 2022).

The  $\sigma^S$ , also known as  $\sigma^{38}$ , is responsible for the generalised stress response and directs the RNA polymerase to genes upon conditions of growth arrest, starvation and stress (Nyström, 2004). In contrast with the housekeeping sigma factor, the  $\sigma^S$  has the lowest affinity to core-RNAP and activates only 10% of the bacterial genome. (Österberg, 2011; Sharma, 2010; Baptista et al., 2022). Considering this sigma is required for stress response,  $\sigma^S$  and the other alternative sigma factors tend to win the competition for available core-RNAP in the stationary growth phase (Baptista et al., 2022). In this case, the levels of  $\sigma^S$  increase to 30% of the  $\sigma^D$  levels (Sharma, 2010). Although the levels of  $\sigma^S$  increase during the stationary phase, some  $\sigma^D$ -dependent genes continue to be transcribed (Farewell, 1998).

### 1.3 General trade-off between growth and maintenance

Every living organism has a limited amount of metabolic (including energetic) resources that can be used for two main functions, growth (reproduction) and maintenance (survival) (Nyström, 2004). The distribution of these resources depends mainly on the environment: when conditions are favourable, growth is prioritised, and when they are not, the allocation to survival is preferred (Nyström, 2004). These environmental conditions can be related to temperature, pH, osmolarity, and availability of nutrients, among others (Battesti, 2011).

The RNAP is one of these resources to trade-off between growth and maintenance (Nyström, 2004). Considering that the number of core-RNAP molecules inside the cell is limited, the trade is a consequence of the availability and allocation of the core-RNAP through sigma factors competition (Sharma, 2010; Nyström, 2004). If environmental conditions changes, the allocation must change as well. In the transition from nutrient abundance to nutrient starvation, for example, the amount of RNAP must be redistributed to transcribe fewer genes involved in growth and more related to maintenance (Sharma, 2010).

This allocation (and, therefore, the competition of sigma factors) has a mediator which regulates the global transcriptional capacity of the cell from growth genes to adaptive survival responses: the alarmone molecule (p)ppGpp (Nyström, 2004; Österberg, 2011).

## 1.4 The regulator guanosine tetraphosphate

The alarmone molecule ppGpp (guanosine tetraphosphate) is the primary mediator of the stringent response, which is the process of amino acid starvation in bacteria that leads to the interruption of rRNA and tRNA synthesis (Kvint, 2000; Österberg, 2011; Sharma, 2010). Although the overall stringent response is complex and involves other targets, the strict control of these two sets of target promoters involves direct modulation of RNAP activity (Roberts, 2009; Hauryliuk et al., 2015). ppGpp interacts directly with RNAP, which can be repressed or activated in a promoter-dependent way (Roberts, 2009; Sharma, 2010). It binds to the  $\beta$  and  $\beta'$  subunits of core-RNAP, preventing it from forming an open complex and inhibiting unnecessary rRNA synthesis during growth arrest (Jishage et al., 2002; Magnusson, 2005; Hauryliuk et al., 2015). Once the complex is inhibited, alternative sigma factors can bind to core-RNAP. Alternative sigma factors compete better in the presence of ppGpp, allowing the cell to respond to growth arrest or different stresses (Jishage et al., 2002; Magnusson, 2005). The  $\sigma^S$ ,  $\sigma^H$ ,  $\sigma^N$  and  $\sigma^E$  require ppGpp for transcription activation (Magnusson, 2005; Potrykus, 2008).

During nutrient abundance, the levels of ppGpp are low and during starvation, inactive ribosomes resulting from a lack of amino-acylated tRNAs induce the production of (p)ppGpp (Hauryliuk et al., 2015; Nandy, 2022). If ppGpp cellular levels are high, this signals nutrient stress, leading to adjustments in gene expression (Potrykus, 2008). However, the same high levels without starvation can quickly inhibit growth and protein synthesis of exponentially growing *E. coli* cells (Potrykus, 2008). It is established that in

*E. coli*, the complete elimination of (p)ppGpp can lock cells in growth mode, ignoring any environmental change (Potrykus, 2008).

ppGpp can also be a positive effector of gene expression since some  $\sigma^D$ -dependent promoters require this molecule for their induction during growth (Jishage et al., 2002; Potrykus, 2008).

Since ppGpp is a regulator of sigma factors competition, it is known as a master transcription regulator (Jishage et al., 2002; Nandy, 2022). However, ppGpp alone cannot efficiently cause destabilisation of promoters; it needs a cofactor: the DksA protein, which is also an anti-sigma factor (Roberts, 2009). DksA is also required for stringent response and, together with ppGpp, stimulates the accumulation of  $\sigma^S$  during early stationary phase (Kvint, 2000; Potrykus, 2008).

## 1.5 Anti-sigma factors

Considering that  $\sigma^D$  is present in the cell at a higher concentration and has the highest affinity to core-RNAP, bacteria use many strategies to diminish the transcriptional ability of this sigma factor to allow the cell to respond to stress (Sharma, 2010). Despite the increase of  $\sigma^S$  during the stationary phase, the higher levels alone cannot compensate for the lowest affinity to core-RNAP, which is why the anti-sigma factors molecules are necessary (Sharma, 2010).

The anti-sigma factors are proteins which bind to a specific sigma factor and inhibit its activity (Sharma, 2010). Therefore, the anti-sigma factors control the availability of the alternative sigma factors (Österberg, 2011). Many anti-sigma molecules and different mechanisms modulate the activity of sigma factors, including phosphorylation-activated binding to a partner protein that tags the sigma for destruction (Österberg, 2011).

The Rsd protein (regulator of sigma D) is an anti-sigma factor repressor of  $\sigma^D$  (Piper et al., 2009; Sharma, 2010). This protein binds to  $\sigma^D$  in the stationary phase and forms a complex, reducing the availability of this sigma factor which facilitates the formation of alternative holoenzymes (Battesti, 2011; Österberg, 2011). Therefore, through this process, Rsd facilitates the distribution of core-RNAP to alternative sigma factors, including  $\sigma^S$  (Jishage et al., 2002; Sharma, 2010). Although Rsd has important anti-sigma activity, this definition is not entirely appropriate since this protein can be overexpressed without interfering with cell growth (Österberg, 2011).

Another anti-sigma molecule is the Crl protein, that when attached to  $\sigma^S$ , facilitates the sigma factors' competition in favour of  $\sigma^S$  (Österberg, 2011; Zhao et al., 2019). This protein is expressed constitutively and is required for maximal expression of  $\sigma^S$ -dependent promoters, but it does not affect  $\sigma^S$  levels (Battesti, 2011).

The protein DksA is also an anti-sigma factor, which can inhibit transcription directly by binding to  $\sigma^D$  or indirectly by altering the core binding competitiveness of sigma factors (Potrykus, 2008; Sharma, 2010). In *E. coli*, the levels of DksA are relatively constant (Österberg, 2011). This anti-sigma molecule is involved in increasing  $\sigma^S$  levels during the stationary phase, together with ppGpp (Bernardo et al., 2006; Potrykus, 2008; Sharma, 2010). Both DksA and ppGpp act together during stringent response and facilitate the switchover of transcription during starvation (Sharma, 2010).

6S RNA is also an anti-sigma factor which negatively affects  $\sigma^D$ -RNAP holoenzyme, binding to it and turning into an inactive form (Battesti, 2011). This regulatory RNA binds to the holoenzyme RNAP attached with  $\sigma^D$  but not with core-RNAP or  $\sigma^D$  alone (Sharma, 2010). The function of 6S RNA is to increase  $\sigma^S$ -dependent promoter transcription (Battesti, 2011). Therefore, it accumulates during the stationary phase (Sharma, 2010).

Besides the anti-sigma, other factors interfere in transcription mediation by sigma factors, like the supercoiling status of DNA or chemical substances, like acetate and potassium glutamate (Sharma, 2010). The negative supercoiling usually favours  $\sigma^D$ , and relaxed DNA favours  $\sigma^S$ -dependent promoters (Sharma, 2010).

## 1.6 Regulation of alternative sigma factors

Regulation of alternative sigma factor activity is usually complex, with multiple tiers of control to regulate both their expression levels and activities (Österberg, 2011). The alternative sigma factors frequently are under tight negative regulation to avoid their competition for core-RNAP in conditions that they are not required (Battesti, 2011).

The stress response sigma factor  $\sigma^S$  is involved in the regulation of approximately 500 genes and the gene RpoS itself is regulated by many factors (Brown et al., 2002; Kim, 2020). The regulation of  $\sigma^S$  expression involves three different levels: transcriptional, translational and protein stability (Battesti, 2011; Kim, 2020). During transcription, the high levels of (p)ppGpp have an increasing effect on  $\sigma^S$  mRNA levels, suggesting a stimulatory effect of transcription (Battesti, 2011). During translation, the long 5' UTR of  $\sigma^S$  transcript folds into a stem-loop that obstructs the ribosome binding

site, which decreases translation of  $\sigma^S$  (Battesti, 2011). Furthermore, there are small RNAs (sRNAs) that activate the RpoS gene at the post-transcriptional level by directly base-pairing with  $\sigma^S$  mRNA (Kim, 2020). These sRNAs stimulate RpoS translation by unfolding the  $\sigma^S$  mRNA 5' UTR, exposing the translation start site of RpoS that was blocked by a folded stem-loop structure in the 5' UTR (Kim, 2020). The proteolytic regulation level involves the targeted degradation of  $\sigma^S$  by a protease and is one of the major examples of regulated proteolysis in *E. coli* (Battesti, 2011).

The regulation of  $\sigma^S$  activity involves the competition between sigma factors, the antisigma and regulatory molecules activity and the transcription of genes activated by  $\sigma^D$  and  $\sigma^S$ , and also  $\sigma^S$  exclusively (Battesti, 2011).

### 1.7 Persister cells

Persister cells are slow-growing variants of regular cells highly tolerant to antibiotics or other kinds of stress (Lewis, 2010). They represent a health threat due to the possibility of causing recurrent infections from many diseases since they are tolerant to antibiotics (Radzikowski et al., 2016). Persisters can enter a non-growing state before an antibiotic treatment starts, and they cannot proliferate in the presence of the antibiotic, considering they are not resistant but tolerant to antibiotics (Kaldalu et al., 2020).

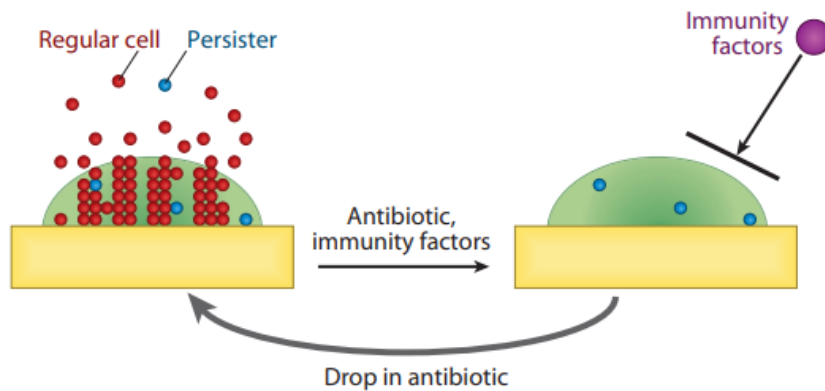


**Figure 3** - Schematic representation of why persister cells are a health threat (Lewis, 2010)  
 Persister cells represent a health threat due to the possibility of causing recurrent infections from many diseases since they are tolerant to antibiotics (Radzikowski et al., 2016).

Persister cells have higher SOS response, cold/hot shock, and toxin/antitoxin systems (TAS), as well as lower levels of flagellum-related transcripts compared to growing cells (Radzikowski et al., 2016).

It is not well established in literature what triggers persistence, and many mechanisms involved in the induction and regulation of this process have not been fully understood yet. (Radzikowski et al., 2016; Miyaue et al., 2018). However, there is evidence that both starved and persister cells must be caused by a common cue (Radzikowski et al., 2016). Persisters have higher levels of proteins required for stress response, including starvation response, RNA catabolism, DNA repair and protein folding (Radzikowski et al., 2016). Persister cells can also be formed stochastically in microbial populations as a survival strategy to respond to dynamic and stressful environments, but spontaneous persisters are less common than triggered persisters (Lewis, 2010; Kaldalu et al., 2020; Nandy, 2022). Low concentrations of antibiotics like fluoroquinolones and aminoglycosides can also trigger persistence formation (Kaldalu et al., 2020). Other environmental conditions are thought to enhance persister formation, such as diauxic shift, extreme pH and DNA damage (Fisher, 2017).

Nutrient shifts can also lead to persistence, generating cells with enhanced antibiotic tolerance and increased ppGpp levels that operate their metabolism optimised for energy generation and not cellular growth (Amato, 2014; Radzikowski et al., 2016). In case nutrient availability is not ideal, cellular resources are allocated to express stress-response proteins instead of proteins required for rapid growth, reducing the growth rate (Nandy, 2022).

Considering the stress response is high in persisters,  $\sigma^S$  is a good candidate for responsible for inducing persisters formation (Radzikowski et al., 2016).  $\sigma^S$  levels are elevated in persisters cells, and it was found that  $\sigma^S$  is primarily responsible for the proteome of persisters (Radzikowski et al., 2016). Therefore, the cue for entering the persister state in nutrient-rich conditions must be the same as for entering starvation, in which  $\sigma^S$  and ppGpp play a role in this process, but what is triggering this mechanism is still a question (Radzikowski et al., 2016).

The alarmone (p)ppGpp was also thought to be involved in persister formation, considering its role in stringent response regulation (Fisher, 2017; Hauryliuk et al., 2015). However, this could not be confirmed since the absence of (p)ppGpp in the cell leads to a decreased number of persisters but not a complete lack of formation (Fisher, 2017).

## 2. Objectives

The aim of this study was 1- to measure the gene expression of constitutive sigma factor  $\sigma^D$  and stress response sigma factor  $\sigma^S$ , to understand better the trade-off between the sigma factors and core RNA Polymerase; 2- to test the hypothesis that under growth-supporting conditions, a small population of cells is already expressing more sigma  $\sigma^S$ , thus preparing for more stressful conditions and 3- to understand how important sigma  $\sigma^S$  is to persister cells formation.

For this purpose, specific objectives were established:

- To make an *E. coli* strain using CRISPR-Cas9-based genetic engineering with fluorescent reporter constructs after the promoters of  $\sigma^D$  (red) and  $\sigma^S$  (green), with both colours on the same cell.
- To test the constructed strain containing the fluorescent reporters using flow cytometry (single-cell level) and plate reader (average population cell level) experiments.
- To test the constructed strain containing the fluorescent reporters using flow cytometry under growth-supporting and stress-inducing conditions.



## 3. Materials and Methods

### 3.1 Bacterial strain and growth conditions

The bacterial strain used in the genome engineering procedures was *Escherichia coli* MG1655. For transformations, high efficiency 5-alpha competent cells C29871 (NEB) were used as a cloning host, genotype *fhuA2 Δ(argF-lacZ) U169 phoA glnV44 Φ80 Δ(lacZ)M15 gyrA96 recA1 relA1 endA1 thi-1 hsdR17*. Cells were cultured in Lysogeny Broth (LB also known as Luria Broth or Luria-Bertani) medium and M9 minimal medium without amino acids and supplemented with 0.4% glucose aerobically at 37 °C under agitation.

### 3.2 Plasmids

The plasmids containing the genes of the fluorescent reporters pDRF1-GW were kindly provided by Bas Teusink (Botman et al., 2019). The plasmids pCas and pTargetF, containing the Cas9 protein and the homologous recombination region, respectively, were provided by Sheng Yang (Jiang et al., 2015).

All plasmids were purified from maintenance strain using EZNA<sup>®</sup> plasmid isolation kit (Omega Bio-tek) according to the manufacturer's instructions (Farnelid et al., 2013). This process is based on the alkaline-lysis method of the cell, followed by binding, washing, and eluting the DNA from the silica mini spin column (HiBind<sup>®</sup> mini-column).

Two pTargetF plasmids were designed: one containing the red fluorescent protein mScarlet1 gene to be inserted downstream  $\sigma^D$  and the other containing the green fluorescent protein mNeonGreen gene to be inserted downstream  $\sigma^S$ , both with the same ribosome binding site.

The designed plasmids were used in the two-plasmid system for genome editing adapted from Jiang *et al.* (2015). In this system, the Cas9 enzyme is directed by sgRNA to the target region (N20 region). After being degraded by Cas9, the region is repaired by the Homologous recombination region (HR region), containing a fragment of the gene sequence, including the degraded fragment, and the gene of fluorescent reporters for being inserted.

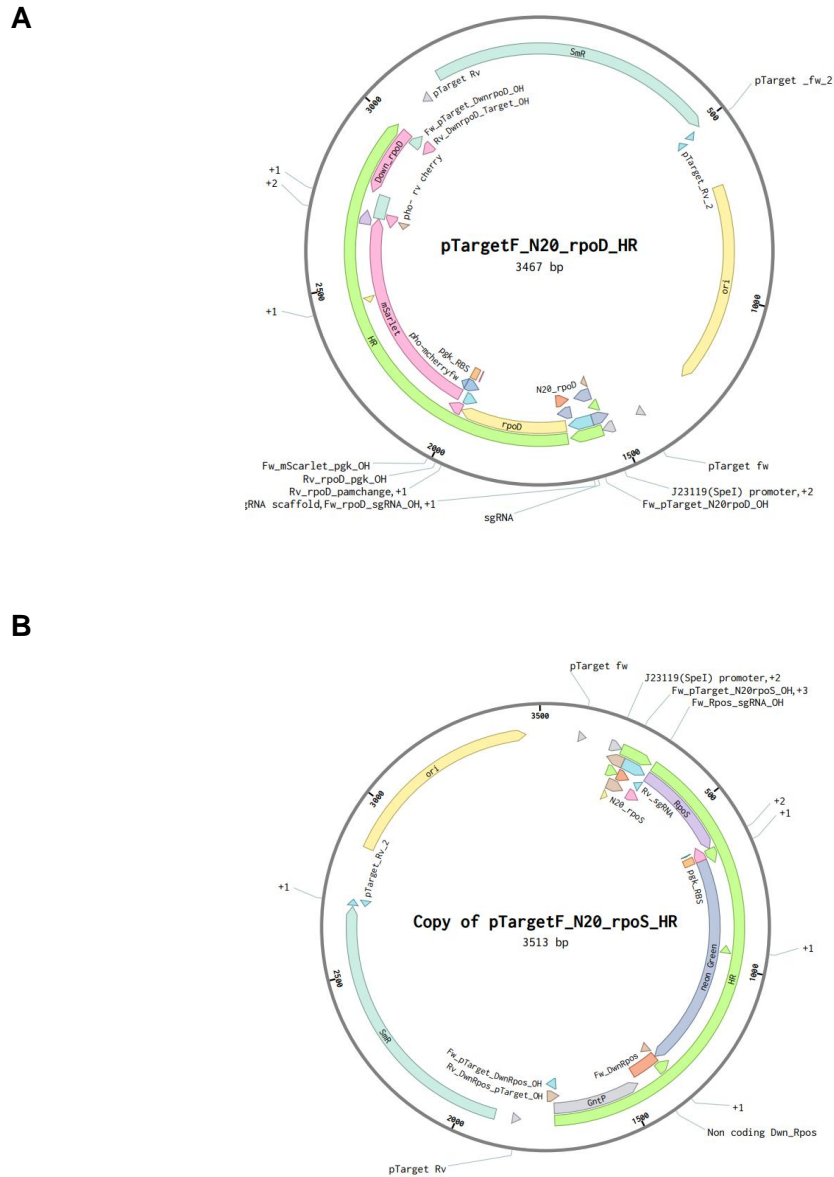


**Figure 4** - Schematic representation of the designed pTargetF plasmids for Crispr-Cas9 two-plasmid system for (A) *rpoD* gene and (B) *rpoS* gene

The Homologous recombination region (HR region) is used to repair the cut by Cas-9, containing a fragment of the gene sequence, including the degraded fragment, and the gene of fluorescent reporters for being inserted. For *rpoD* gene, the red reporter *mScarlet* gene was inserted into the plasmid, and for *rpoS* gene, the green reporter *mNeonGreen* gene was inserted into the plasmid. N20 is a 20-bp region complementary to the cut target fragment for both plasmids.

To construct each plasmid, first, the N20 region was introduced by PCR and Gibson assembly, and then the HR region was inserted with the reporter's gene, using the same method. All PCR primers were designed with overlap endings, meaning that all fragments have a sequence of overlap with the fragment right next to them, which enables the fusion of the fragments either by PCR or by Gibson assembly.

To construct the HR region, genomic DNA was extracted from a 10 mL overnight culture of MG1655 (LB medium, 37 °C, 200 rpm). Genomic DNA extraction was performed using the GenElute bacterial genomic DNA kit (Sigma-Aldrich), following instructions from the manufacturer. This procedure is based on the lysis of the cell,

followed by binding, washing, and eluting the DNA from a silica spin column. Phusion Hot Start II Polymerase (Thermo Scientific™) PCR was performed in the genomic DNA to amplify the HR region and create two different fragments of the designed pTargetF plasmid. The third fragment was also created with Phusion PCR, using the plasmids containing the fluorescent proteins as a template.

N20 and HR regions were introduced on pTargetF by PCR using Phusion Hot Start II Polymerase (Thermo Scientific™). The primers used are listed in supplementary table 1. A temperature of 60 °C was used for annealing the primers and the elongation step was 40 seconds. All the PCR products were confirmed by electrophoresis in 1% agarose gel with 1X TAE buffer and ethidium bromide 0.2 µg/mL. The gel was run at 100 V for one hour.

All the amplified fragments were cut from the agarose gel and purified using EZNA® gel extraction kit (Omega Bio-tek), according to the manufacturer’s instructions (Liu et al., 2012). Except for the elution buffer, which was added a lower amount to achieve a higher DNA final concentration. After purification, the fragments were attached by Gibson assembly reaction, performed with 1 pmol of each fragment DNA (1:1 molar ratio) and 2X Gibson assembly mix (NEB®), incubated at 50 °C for 60 minutes.

Afterwards, the product of this reaction was used to transform *E. coli* competent cells by heat shock method. 5 µL of the plasmid DNA obtained from the Gibson assembly was incubated with chemically competent cells for 10 minutes on ice, then put in a bath at 42 °C for 30 seconds, and then immediately put on ice again. The cells were recovered in 1 mL of SOC medium for one hour at 37 °C and 200 rpm and then plated on LB agar plates supplemented with spectinomycin (50 µg/mL). The plates were incubated at 37 °C overnight.

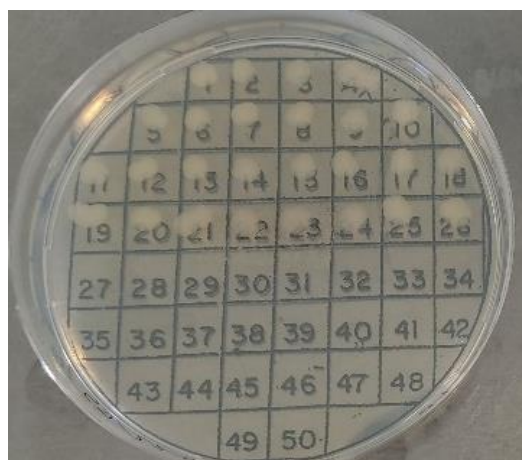


**Figure 5** - LB plate from colony PCR *E. coli* high efficiency 5-alpha competent cells transformants in LB plate supplemented with 50 µg/mL spectinomycin.

Positive clones were confirmed by colony PCR, using GoTaq Polymerase master mix (Promega), and cultured in 10 mL of LB medium supplemented with spectinomycin (50 µg/mL) overnight, at 37 °C and 200 rpm. Plasmid isolation was performed using the same kit, and each sample of purified plasmid DNA was sent for DNA sequencing to confirm the correct insertion of the sequence of interest.

### 3.3 Genome insertion of fluorescent reporters

To insert the fluorescent reporters in *E. coli* MG1655 chromosome downstream the sigma factors  $\sigma^D$  and  $\sigma^S$  genes, the two plasmids CRISPR-Cas9 method (Jiang et al., 2015, Kang et al., 2022) was performed. Firstly, competent cells were transformed with pCas plasmid. MG1655 cells were pre-cultured in 10 mL of LB at 37 °C and 200 rpm overnight and diluted 80 times in the morning. The diluted culture was regrown until  $OD_{600nm}$  0.6 at the same conditions. Once this OD value was reached, cells were washed with cold, sterile deionised water and spun down at 4 °C, four times to wash the salts and make them electrocompetent. Afterwards, cells were resuspended in 150 µL of deionised water.

These cells were transformed with pCas plasmid by electroporation. The cells and isolated pCas were transferred into a 0.1 cm electroporation cuvette previously cold and pulsed for 5 milliseconds. Transformed cells were recovered in 1 mL of SOC medium for one hour at 30 °C and 200 rpm, then plated on LB agar plates supplemented with kanamycin (50 µg/mL). The plates were incubated at 30 °C overnight (because pCas is temperature sensitive).

Transformants clones were pre-cultured in LB supplemented with kanamycin (50 µg/mL) at 30 °C and 200 rpm overnight. This overnight culture was diluted 80 times in the same medium and was regrown until  $OD_{600nm}$  0.3 under the same conditions. At this point, arabinose was added to reach a final concentration of 10 µM. When the  $OD_{600nm}$  reached 0.6, cells were washed with cold, sterile deionised water and spun down at 4°C to wash the salts and make them electrocompetent. This process was repeated four times. Afterwards, cells were resuspended in 150 µL of deionised water. These cells were transformed with pTargetF plasmid by electroporation, following the same procedure described above. Recovered cells were plated in LB plates supplemented with kanamycin (50 µg/mL) and spectinomycin (50 µg/mL).

Positive clones were confirmed by colony PCR, using primers outside the HR region inserted on the pTargetF plasmid to ensure the primers would anneal in genomic DNA.

These transformants were cultured overnight in LB supplemented with kanamycin (50 µg/mL) and IPTG (1mM) for pTargetF curing.

The IPTG cultures were diluted in 1X PBS to check the OD<sub>540nm</sub>. After this, the cultures were diluted 350 times and plated on LB plates supplemented with kanamycin (50 µg/mL) to create single colonies. The plates were incubated at 30 °C overnight. On the next day, each colony from these plates was streaked in LB plates with kanamycin with a grid on it and also in LB spectinomycin plates with a grid on it, in the same position. The plates were incubated at 30 °C overnight. Cells that grew on kanamycin while corresponding cells did not grow on spectinomycin have lost the pTargetF plasmid and were used for proceeding.

The pTargetF cured cells were cultured overnight at 37°C in 2 mL of LB with no antibiotics to lose the pCas plasmid. The same procedure was repeated to create single colonies of these cultures and test for pCas lost. The single colonies were streaked in LB plates without any antibiotics with a grid on them and also in LB kanamycin plates with a grid on them, in the same position. The plates were incubated at 37 °C overnight. Cells that grew on LB while corresponding cells did not grow on LB containing kanamycin have lost the pCas plasmid and were used for proceeding.

The pCas cured cells were cultured overnight in 10 mL of LB with no antibiotics at 37°C and 200 rpm. Glycerol stocks were made from this culture and stored at -80 °C. The strains created from this process were tested in growth experiments.

To confirm the correct insertion of the reporters, genomic DNA was extracted from overnight cultures using EZNA<sup>®</sup> Bacterial DNA kit, following instructions from the manufacturers (Gulitz et al., 2011). The kit procedure is based on the lysis of the cell by Lysozyme followed by digestion using RNase and then binding, washing, and eluting DNA using a mini silica spin column.

PCR was performed using the extracted DNA. The last 400 bp of both sigma factors genes, the fluorescent protein gene, and approximately 400 bp after the fluorescent protein's genes were amplified to make sure the insertion was in the right place (figure 6). Phusion PCR was performed (Thermo Scientific<sup>™</sup>). A temperature of 60 °C was used for annealing the primers and the elongation step was 40 seconds. 30 cycles were used.

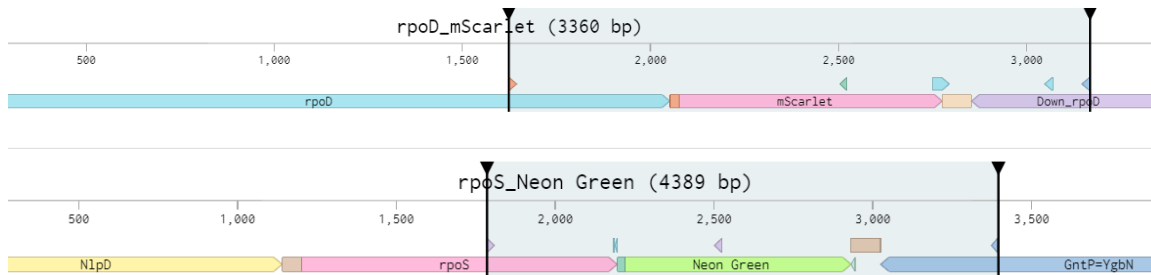


**Figure 6** – Schematic gene representation of the fluorescent reporter genes insertions in *E. coli* genome downstream the housekeeping sigma factor  $\sigma^D$  and the stress response sigma factor  $\sigma^S$ . The blue fragment above represents *rpoD* gene and right after, the pink fragment represents *mScarlet* red reporter gene. The pink fragment below represents *rpoS* gene and right after, the green fragment represents *mNeonGreen* green reporter gene. In both cases, the selected region was amplified with Phusion PCR to make sure the insertion was correct in *E. coli* genome.

The PCR products were confirmed by electrophoresis in the same conditions described previously. The amplified fragments were cut from the agarose gel, and each purified fragment was sent for DNA sequencing.

### 3.4 Microscopy imaging

The generated strains were checked in the fluorescence microscope using agarose pads (1.5% agarose in M9 minimal medium). Overnight cultures from constructed strains and wild type (as control) were diluted in fresh minimal medium and regrown for 3 hours. 6  $\mu$ L of each culture was placed between the agarose pad and a coverslip. Fluorescent signals were visualised on a Nikon Ti-Eclipse microscope with an Andor Zyla 5.5 sCMOS Camera and a SOLA 6-LCR-SB power source using a GFP-B filter cube (470/40 excitation filter, 505 nm LP dichroic mirror, 535/50 emission filter) for the green reporter and a mCherry filter cube (562/40 excitation filter, 593 nm LP dichroic mirror, 640/75 emission filter) for the red reporter (Botman et al., 2019). Microscopy images were taken with 200 milliseconds and 2 seconds of exposure.

### 3.5 Growth experiments

The constructed strains were tested in experiments in which fluorescence was measured during growth to follow sigma factors expression. Wild-type fluorescence was measured as a control.

### 3.5.1 Sigma factors expression at average population cell level

To measure sigma factors gene expression at an average population cell level, a plate reader experiment was performed in the FLUOstar Omega plate reader (BMG Labtech) using the constructs and *E. coli* wild type. For this experiment, cells were pre-cultured in M9 medium overnight and diluted 100 times in fresh medium, and then the plate was filled with these cultures. The schematic representation of the plate layout is in figure 7 below.

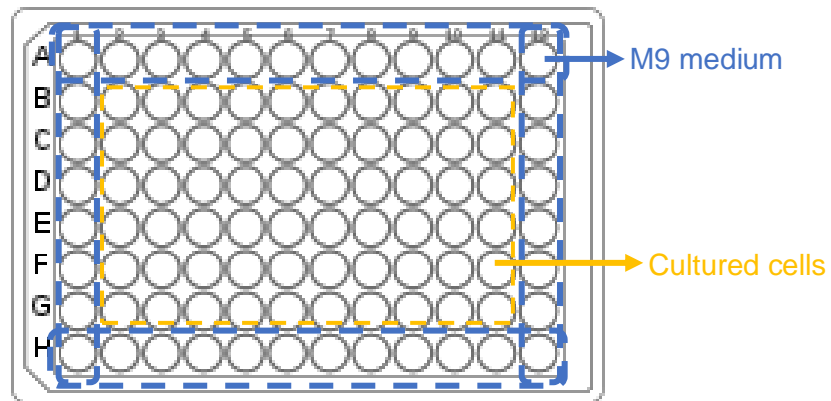


**Figure 7** - 96-well-filled plate layout for plate reader experiment  
M9 medium wells are in blue and bacterial cultures are in yellow. The two different strains and wild type were filled randomly in the yellow area

The plate was sealed with parafilm and incubated for 48 hours. Bacterial growth was measured by  $OD_{600nm}$  reading and the fluorescence signal was measured at 561 nm for the red reporter and 488 nm for the green reporter.

### 3.5.2 Sigma factors expression at single cell level

Flow cytometry experiments were performed in the CytoFLEX flow cytometer (Beckman Coulter) to measure sigma factors gene expression at a single cell level, using the constructs and *E. coli* wild type. Cells were pre-grown overnight in minimal media M9 and diluted. The diluted cultures were grown until exponential phase OD value and then diluted again to  $OD_{600nm}$  0.2. From this point, measurements were taken every 30 minutes until the stationary phase was reached. Wild-type fluorescence was measured to correct the background fluorescence from the reporter system.

To take the measurements, cells were diluted into pre-warmed fresh M9 medium and vortexed for 10 seconds. For each strain, biological replicates were performed, acquiring 20  $\mu$ L of fixed volume per measurement. For the GFP signal, 525/40 nm filters

were used for emission and for the RFP signal, 610/20 nm. The FSC-H detection threshold was set at 5000 and the gain at 3000. Events were collected at a flow rate of 10  $\mu$ L/minute.

### 3.5.3 Sigma factors expression in stress-inducing conditions

Flow cytometry experiments were performed using the constructs and *E. coli* wild type in a stress-inducing environment to measure gene expression under these conditions. Firstly, cells were cultured and measurements were taken in the same settings described in the previous section. After three measurements, the culture was spined down at 4000 rpm for 10 minutes. Cells were washed in fresh M9 medium without a carbon source and then transferred to a new flask containing M9 medium with no glucose or any carbon source. New measurements from this culture were taken every 30 minutes in the same acquisition settings.

### 3.5.4 Data analysis

Flow cytometry data were acquired using CytExpert version 2.5 software (Beckman Coulter). The fluorescence data from the Plate reader experiments were acquired by Multi-user Reader Control and MARS Data Analysis software. All the collected data processing was executed in Python, using Jupyter (IPython Notebook, *Anaconda Software Distribution*, Anaconda Inc). Data visualisation was presented using Seaborn and Matplotlib.



## 4. Results

### 4.1 Genome insertion of fluorescent reporters

Fluorescent reporters were inserted in the *E. coli* MG1655 chromosome downstream the sigma factors  $\sigma^D$  and  $\sigma^S$  genes, respectively, using the two plasmids CRISPR-Cas9 method (Jiang et al., 2015; Kang et al., 2022). Firstly, the encoding gene of the red fluorescent protein mScarlet1 was inserted right after the  $\sigma^D$  gene. Once this strain was generated, a second CRISPR-Cas9 system was performed to insert the encoding gene of the green fluorescent protein mNeonGreen after the  $\sigma^S$  gene. Positive clones were confirmed by colony PCR (Figure 8), using primers outside the HR region inserted on the pTargetF plasmid to ensure the primers would anneal in genomic DNA and not on the plasmid that is also present in the cells.

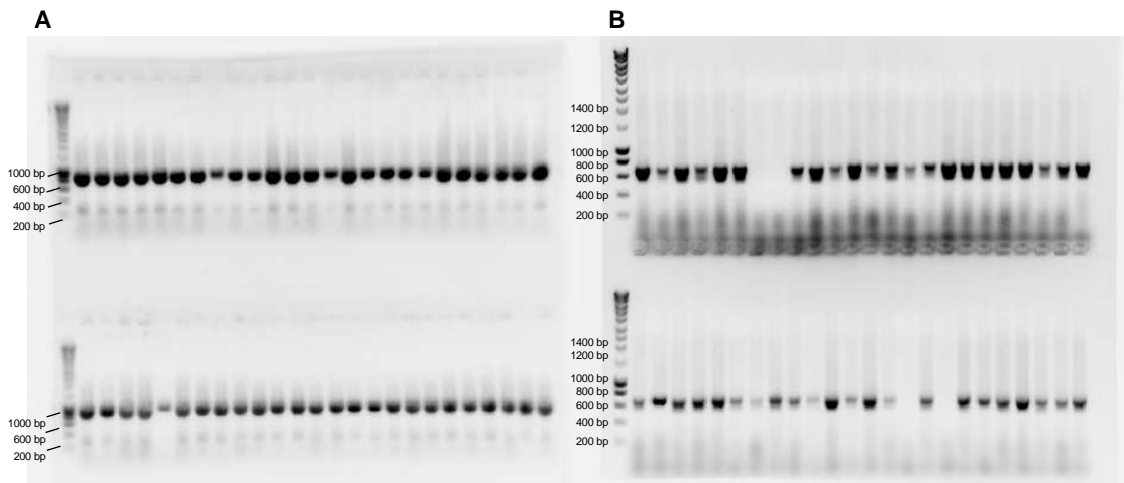


**Figure 8** – Agarose gel electrophoresis analysis of Colony PCR products from *E. coli* MG1655 cells after Crispr-Cas9 system experiments

(A) Clones from the CRISPR-Cas9 experiments to insert the red fluorescent reporter downstream *rpoD* gene in *E. coli* MG1655 genome. Positive clones show a band at 898 bp. (B) Clones from the CRISPR-Cas9 experiments to insert the green fluorescent reporter downstream *rpoS* gene in *E. coli* MG1655 genome. Positive clones show a band at 739 bp.

Following the two-plasmid CRISPR-Cas9 method, the pTargetF plasmid curing was performed by induction of cells with IPTG. The promoter under a *lacI* operon guided the Cas9 enzyme to the replication origin of the plasmid. For the pCas curing, cells were cultured at 37 °C on account of the temperature-sensitive replicon contained in this plasmid. To confirm the colonies curing, the sensitivity of the cells to appropriate antibiotics (50 mg/L) was tested (Figure 9). Cells that grew on kanamycin while corresponding cells did not grow on spectinomycin have lost the pTargetF plasmid and

cells that grew on medium without antibiotics while corresponding cells did not grow on kanamycin were cured of the pCas plasmid.

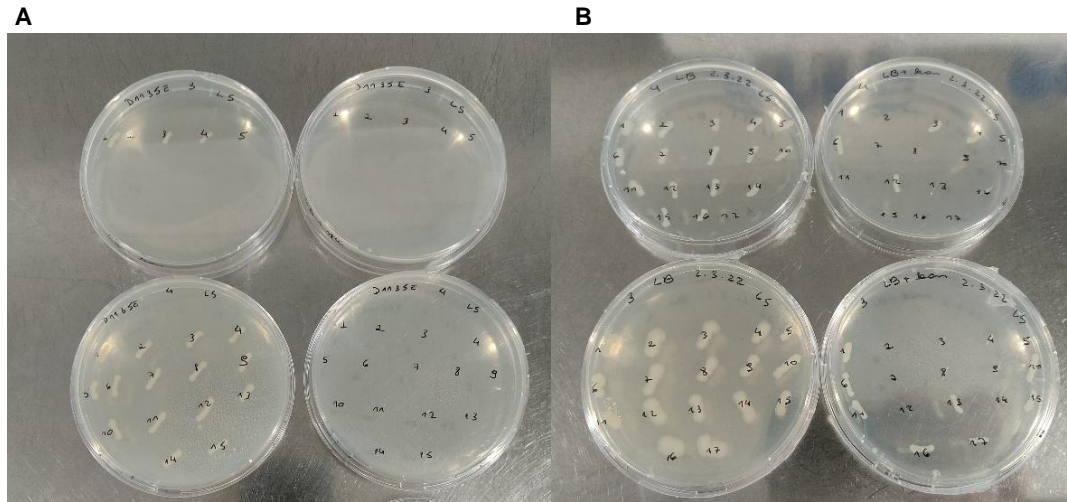


**Figure 9** – *E. coli* MG1655 cells curing from the CRISPR-Cas9 plasmids on LB plates supplemented with antibiotics. (A) Colonies that grew on kanamycin while corresponding colonies did not grow on spectinomycin were cured of pTargetF plasmid (B) and colonies that grew on medium without antibiotics while corresponding colonies did not grow on kanamycin were cured of the pCas plasmid.

Two different strains were generated by the CRISPR-Cas9 system: one containing the red fluorescent protein right after the sigma factor  $\sigma^D$  and the other as well having the red fluorescent protein in the same position in the genome but also containing a green fluorescent protein after the sigma factor  $\sigma^S$ . Both insertions were confirmed using PCR and DNA sequencing. The complete sequence of insertion confirmation for both strains can be consulted in the Supplementary material section (Supplementary Table 2 and Supplementary Table 3).

## 4.2 Microscopy imaging

The fluorescence signal from the constructs was captured using fluorescence microscopy. Cells were cultured overnight and after appropriate dilution, transferred to agarose pads. Microscopy images of both generated strains were taken and compared to wild type in the red and green channels (Figure 10). The images revealed the expression of mScarlet1 and mNeonGreen fluorescent reporters in the red and green channels, respectively. The fluorescence signal from the constructed strains can be easily distinguished from the wild type.

In general, it is well known that *E. coli* cells have considerable green autofluorescence (Mihalcescu et al., 2015; Galbusera et al., 2020). It is possible to

confirm this in the wild-type green channel images, the construct containing just the red reporter after the sigma factor  $\sigma^D$ . In contrast, the red autofluorescence in the cells is insignificant.

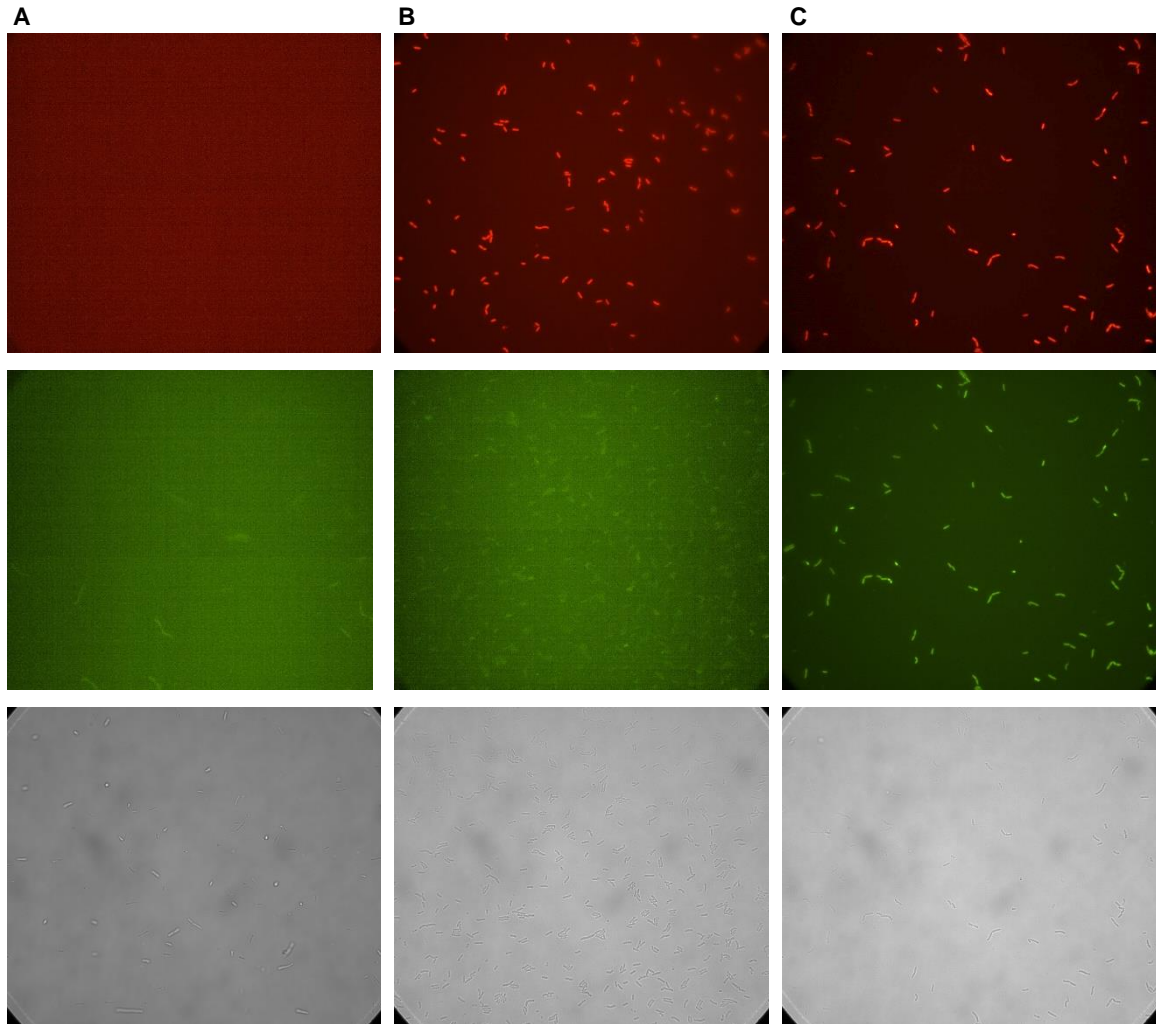


**Figure 10** - Fluorescence microscopy images in the red and green channel and grayscale of *E. coli* MG1655 cells (A) wild-type, (B) strain containing the red reporter after  $\sigma^D$  and (C) the strain containing the red and green reporter after  $\sigma^D$  and  $\sigma^S$ , respectively.

Microscopy images were taken in 1.5% agarose pads with M9 minimal medium, with 200 milliseconds of exposure. Fluorescent signals were visualised on a Nikon Ti-Eclipse microscope with an Andor Zyla 5.5 sCMOS Camera and a SOLA 6-LCR-SB power source using a GFP-B filter cube (470/40 excitation filter, 505 nm LP dichroic mirror, 535/50 emission filter) for the green reporter and a mCherry filter cube (562/40 excitation filter, 593 nm LP dichroic mirror, 640/75 emission filter) for the red reporter.

## 4.3 Growth experiments

### 4.3.1 Sigma factors expression at average cell population level

A plate reader experiment was performed to estimate average population sigma factors gene expression. Cells were grown in a 96-well-plate while measuring  $OD_{600nm}$

and fluorescence signal in the red and green channels. Wild-type fluorescence was measured to establish the background signal from the constructed strains (Figure 11).

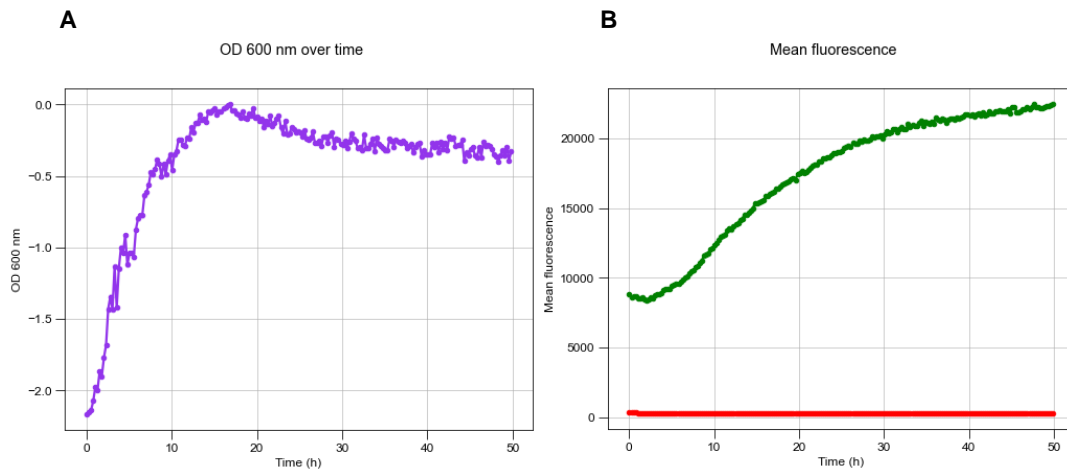


**Figure 11** – *E. coli* MG1655 cell growth and autofluorescence from plate reader experiment, used as control (A) OD<sub>600 nm</sub> measurements of wild-type over time. (B) Wild-type background fluorescence green and red signal measurements over time.

The growth curve from wild-type cells grew exponentially until approximately 18 hours, reaching the OD<sub>600nm</sub> of 1 (Figure 11A). Afterwards, the growth decreased, probably due to nutrient exhaustion. The measured fluorescence confirms that wild-type cells demonstrate quite high green autofluorescence, as stated previously, and almost no red autofluorescence (Figure 11B). Considering that this experiment determines an average population fluorescence, the fluorescence showed an increasing trend corresponding to cell growth. Hence, more cells exhibit more fluorescence.

The fluorescence from the strain containing the red reporter on  $\sigma^D$  was also measured under the same conditions (Figure 12).

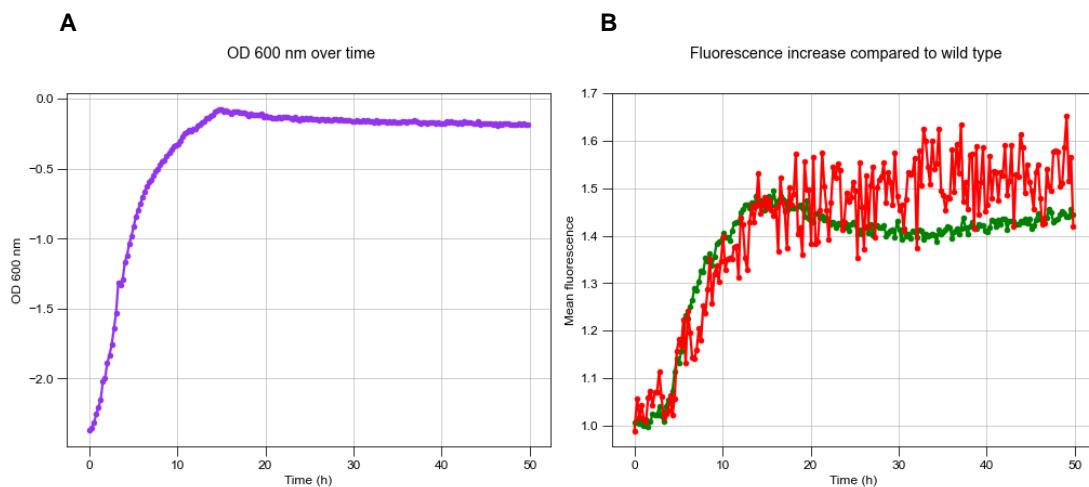


**Figure 12** – *E. coli* MG1655 generated strain containing the single red reporter on  $\sigma^D$  cell growth and sigma factors expression from plate reader experiment (A) OD<sub>600 nm</sub> measured over time and (B) acquired fluorescence signal from the constructed strain compared to wild-type,  $\sigma^D$  expression in red and green autofluorescence from *E. coli*.

The constructed strain cells grew exponentially until approximately 18 hours, after which the OD<sub>600nm</sub> slightly decreased (Figure 12A). Regarding gene expression, the graph was corrected by wild-type background fluorescence. In light of *E. coli*'s high green autofluorescence, the two measured fluorescence signals were too apart from each other. The green signal was substantially higher than the red one, making it difficult to visualise gene expression from the red reporter. Because of this, fluorescence graphs were normalised by dividing the construct fluorescence values by wild-type measured fluorescence values. Therefore, results indicate that the green autofluorescence and the reporter red fluorescence (considering that this strain has just the red reporter) from the construct is higher than wild-type fluorescence (Figure 12B). Results also revealed an increasing trend in the  $\sigma^D$  gene expression in the exponential phase and a constant trend during stationary phase. Results from all replicates can be found in the Supplementary material section (Supplementary figure 1).

Finally, the fluorescence from the strain containing both red and green reporters on  $\sigma^D$  and  $\sigma^S$  was measured (Figure 13).

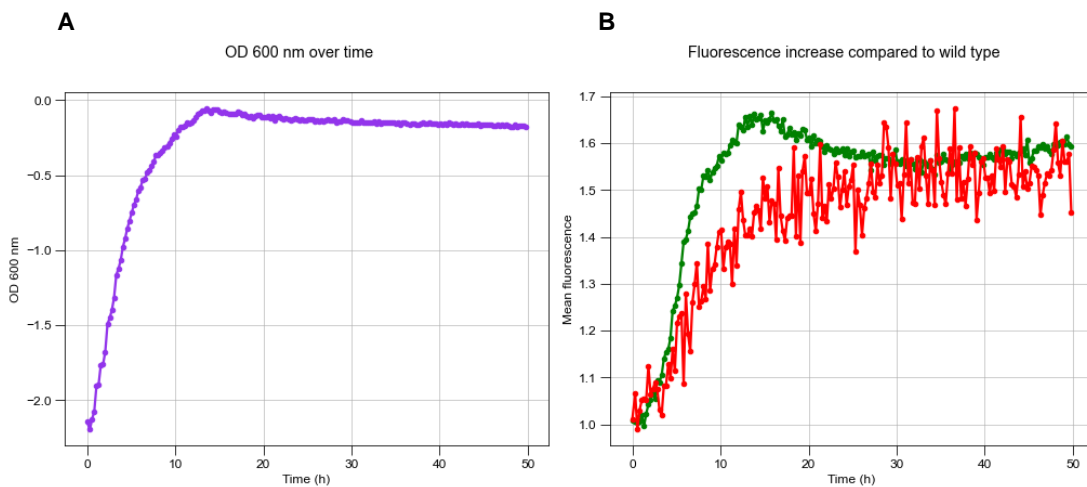


**Figure 13** – *E. coli* MG1655 generated strain containing both red and green reporters on  $\sigma^D$  and  $\sigma^S$  cell growth and sigma factors expression from plate reader experiment  
**(A)** OD<sub>600 nm</sub> measured over time and **(B)** acquired fluorescence signal from the constructed strain compared to wild-type,  $\sigma^D$  expression in red and  $\sigma^S$  expression in green.

The growth curves for this constructed strain indicate a similar growth trend compared to the other constructed strain (Figure 13A). For gene expression, fluorescence graphs were normalised based on wild-type background fluorescence by dividing the construct fluorescence values by wild-type measured fluorescence values, as mentioned previously. These results show an increasing trend in both sigma factors gene expression, especially during the exponential phase (Figure 13B). Therefore, on average, both housekeeping and stress response sigma factors were expressed

similarly during growth, which was not expected considering their function. During the stationary phase,  $\sigma^D$  expression is kept constant and  $\sigma^S$  expression slightly decreases, which is different from expected, considering stress conditions increase during the stationary phase. Compared with the previous strain (Figure 12),  $\sigma^D$  expression shows a similar trend in both cases. The green signal is higher for the strain containing the green reporter in  $\sigma^S$ , as expected, but not substantially higher because of *E. coli*'s high green autofluorescence. Results from all replicates of the constructed strain with reporters on both sigma factors can be found in the Supplementary material section (Supplementary figure 2).

### 4.3.2 Sigma factors expression at single cell level

To investigate sigma factors gene expression at a single cell level, flow cytometry experiments were performed during growth, using the constructs and *E. coli* wild-type cultures. Red and green fluorescence signals were measured on the flow cytometer to follow sigma factors expression and bacterial growth was measured by OD<sub>600nm</sub>.

Wild-type fluorescence was measured during growth to estimate background fluorescence from the constructs (Figure 14).

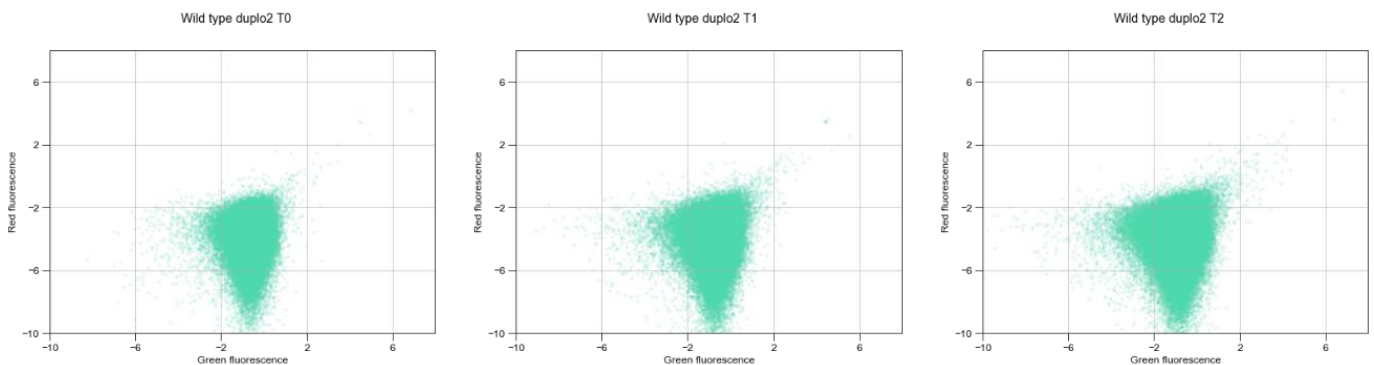


**Figure 14** – *E. coli* MG1655 autofluorescence acquired with flow cytometry, used as control. First three time points of wild-type red fluorescence against green fluorescence signals. Measurements acquired every thirty minutes from early exponential phase culture.

The fluorescence data were corrected by the cell size by dividing the acquired fluorescence values by FSC-A (Forward scatter area) values. The scatter plots show the fluorescence signal of each cell from the culture sample. The cell population growth is noticeable in the plots, and there are no changes in both fluorescence signals. It is possible to see the same pattern for all wild-type measurements. The scatter plots from

all time points acquired from wild-type can be found in the Supplementary material section (Supplementary figure 3).

Density graphs were plotted from the same fluorescence data acquired during growth (Figure 15).

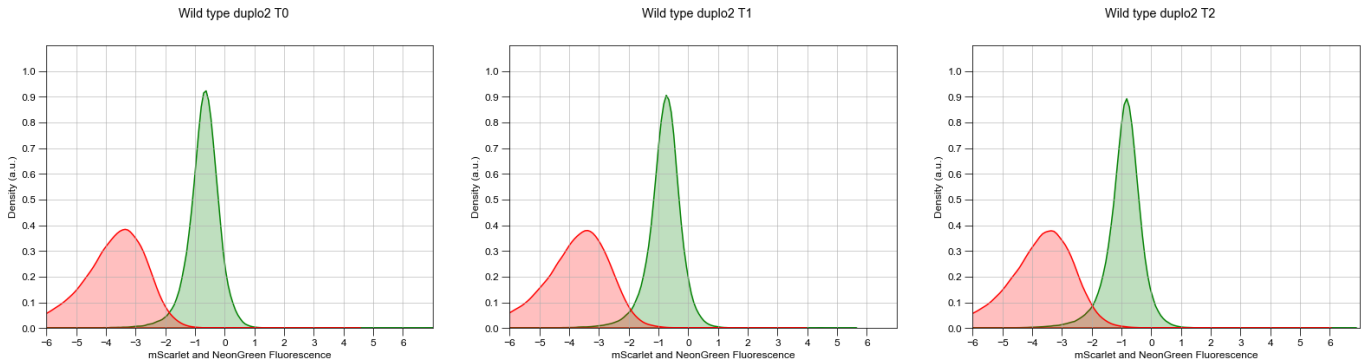


**Figure 15** – *E. coli* MG1655 autofluorescence density plots, acquired with flow cytometry, used as control. Density plots of the first three time points of wild-type red and green autofluorescence signals. Measurements acquired every thirty minutes from early exponential phase culture.

The wild-type fluorescence was kept constant during all measurements and it is possible to see the high green autofluorescence from *E. coli* (Figure 15). Density plots from all measured time points of wild type can be found in the Supplementary material section (Supplementary figure 5).

Flow cytometry results from the strain containing only the red reporter downstream  $\sigma^D$  were not consistent enough.

The fluorescence from the strain containing the red reporter downstream  $\sigma^D$  and the green reporter downstream  $\sigma^S$  was also measured under the same conditions (Figure 16).

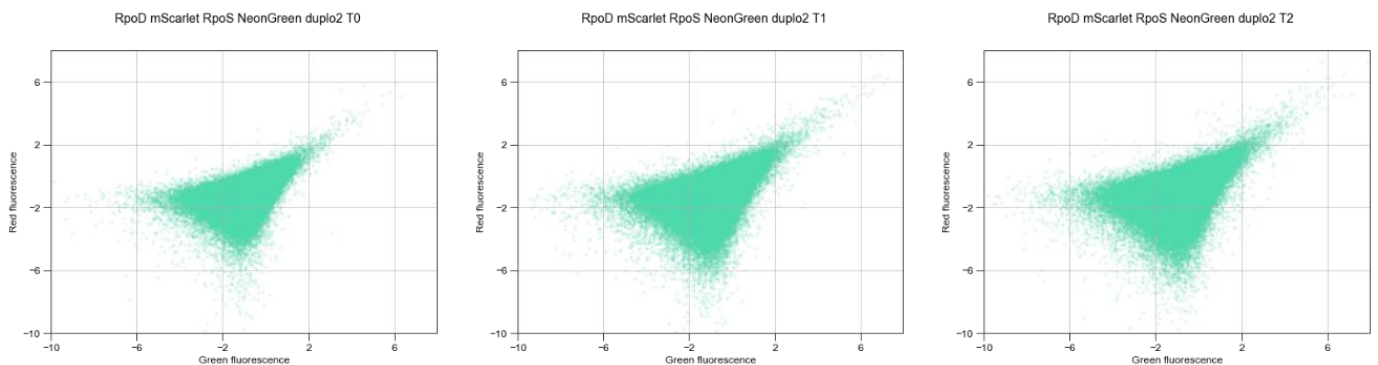


**Figure 16** – *E. coli* MG1655 generated strain containing the red reporter downstream  $\sigma^D$  and the green reporter downstream  $\sigma^S$  fluorescence signal acquired with flow cytometry. First three time points of generated strain, showing red fluorescence against green fluorescence signals. Measurements acquired every thirty minutes from early exponential phase culture.

The fluorescence data were corrected by the cell size by dividing the acquired fluorescence values by FSC-A (Forward scatter area) values. The scatter plots show the fluorescence signal of each cell from the culture sample, and it is possible to see a slight growth through the first three time points (Figure 16). Compared to the wild-type scatter plots, the construct has more red and green fluorescence, as expected. Although the signal for both colours is not substantially higher, the fluorescence signal from the construct is easily distinguished from the wild-type background signal. Results also revealed that the signal for both colours increases over the measurements proportionally, showing no expression of one sigma more than the other. As in the plate reader experiment results, this proportional increase was not expected because of each sigma factor function. All time points acquired from this construct can be found in the Supplementary material (Supplementary figure 4).

Density plots from the same fluorescence data acquired show that the construct fluorescence slightly changed during all measurements (Figure 17). The green signal started high but includes relatively high autofluorescence, and the red signal increases over measurements, reaching out for the green signal. Density plots from all time points of the construct can be found in the Supplementary material section (Supplementary figure 6).

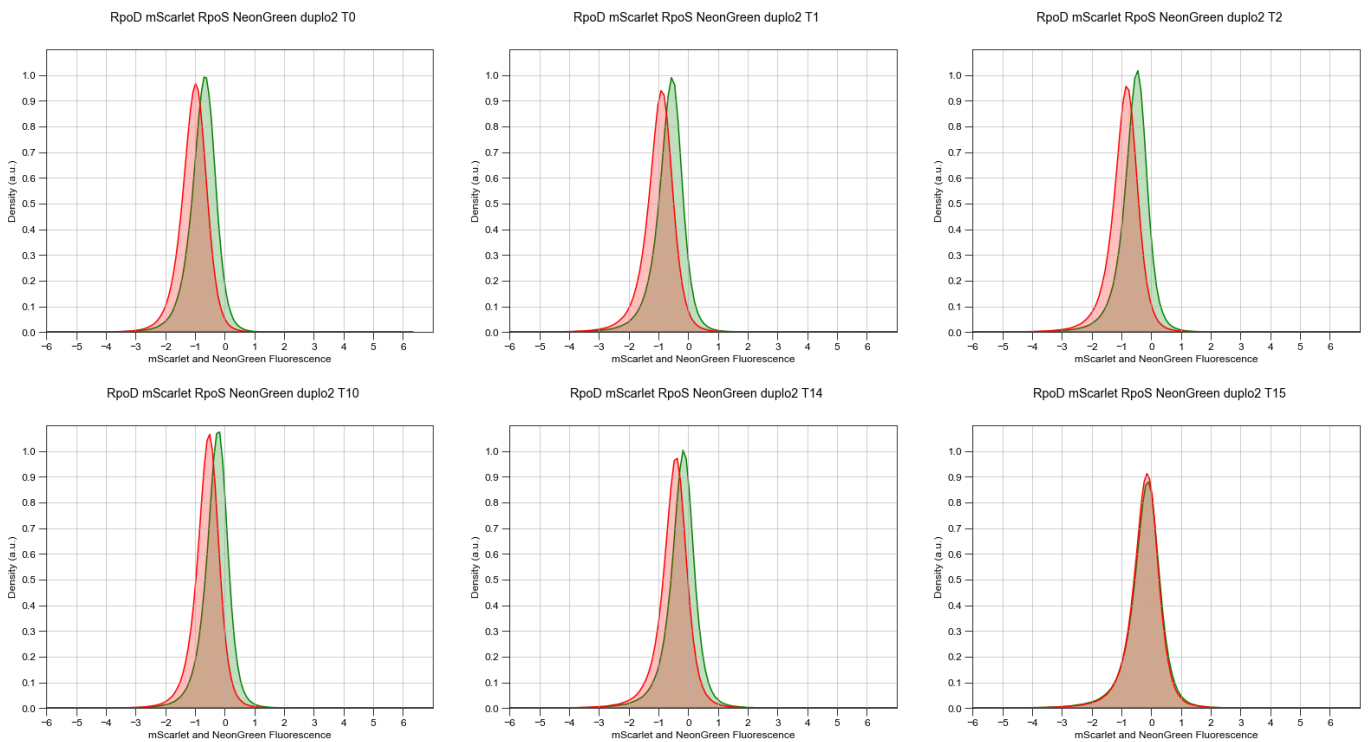


**Figure 17** – Sigma factors expression of *E. coli* MG1655 generated strain containing the red reporter downstream  $\sigma^D$  and the green reporter downstream  $\sigma^S$  in fluorescence density plots, acquired with flow cytometry. Density plots of the first three time points of measurements, acquired during exponential phase followed by the last three time points, in stationary phase. Measurements acquired every thirty minutes from early exponential phase culture.  $\sigma^D$  expression in red and  $\sigma^S$  expression in green.



Considering that it was challenging to interpret the flow cytometry data through the density plots, the average fluorescence from the cell population was calculated for every timepoint and plotted in a new graph (Figure 18).

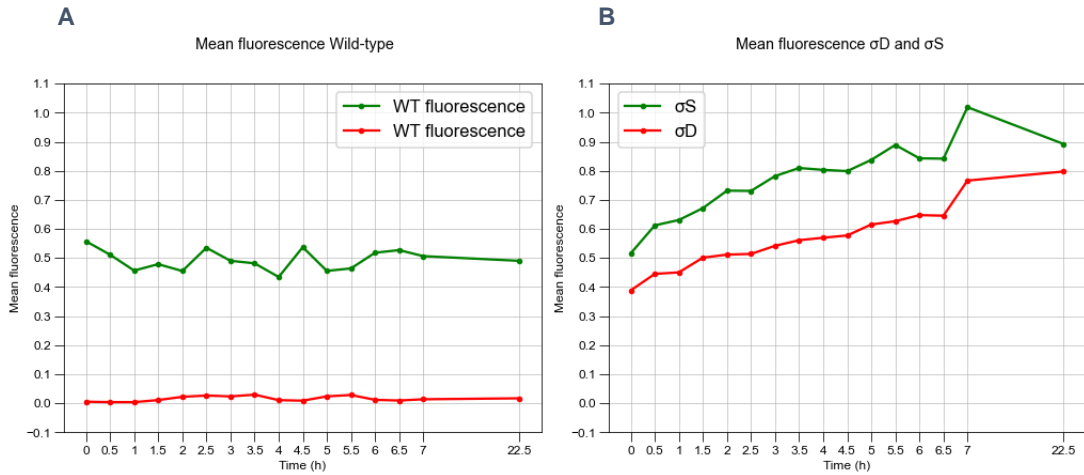


**Figure 18 – (A)** Average autofluorescence of wild-type and **(B)** the average sigma factors expression of *E. coli* MG1655 constructed strain containing the red reporter downstream  $\sigma^D$  and the green reporter downstream  $\sigma^S$ , acquired with flow cytometry

Figure 18A shows the average fluorescence of the wild-type cells over time during flow cytometry measurements. Figure 18B shows the average fluorescence for the construct containing the red reporter on  $\sigma^D$  and the green reporter on  $\sigma^S$  before adjusting for the background fluorescence. The average fluorescence (Figure 19A) was corrected by discounting the fluorescence values of wild-type (Figure 18A) from the construct fluorescence values (Figure 18B).

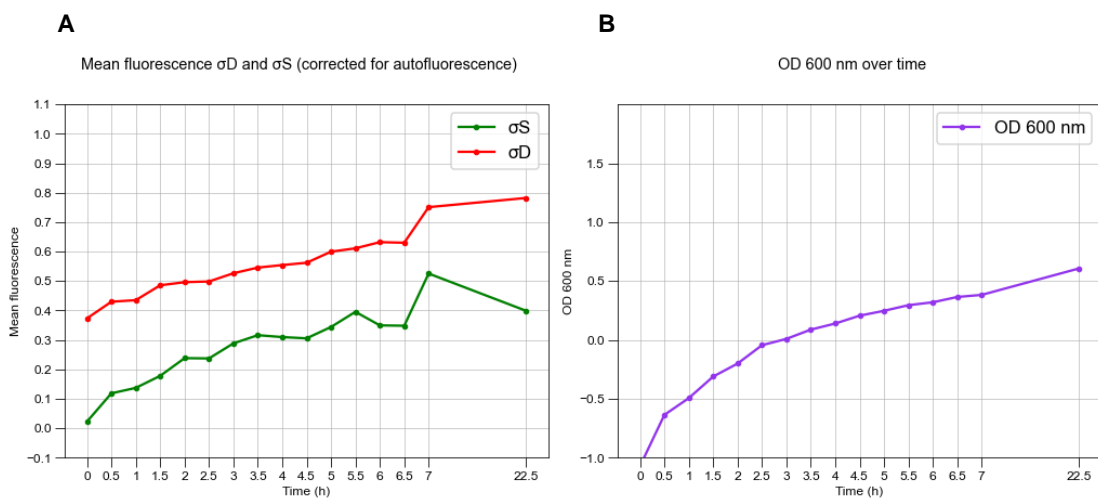


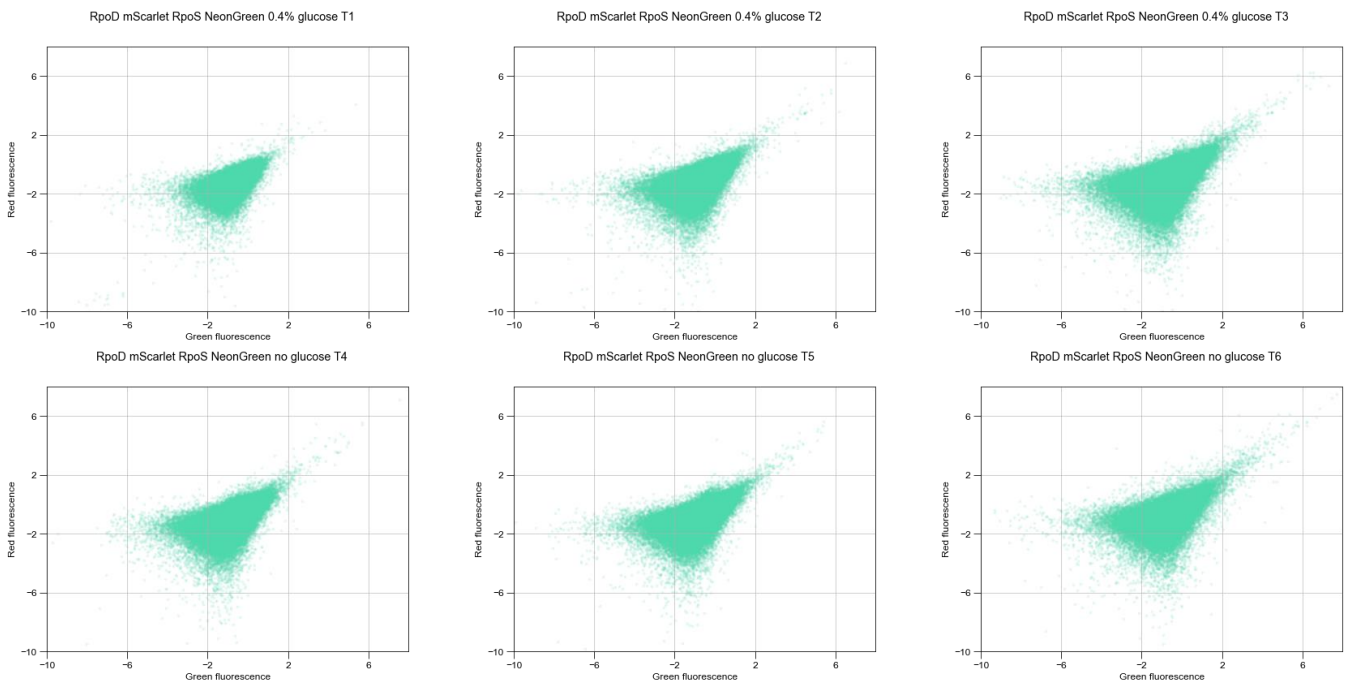
**Figure 19 – (A)** Average sigma factors expression of *E. coli* MG1655 constructed strain containing the red reporter downstream  $\sigma^D$  and the green reporter downstream  $\sigma^S$ , acquired with flow cytometry and corrected by wild-type autofluorescence and **(B)** Cell growth of *E. coli* MG1655 constructed strain containing the red reporter downstream  $\sigma^D$  and the green reporter downstream  $\sigma^S$ .

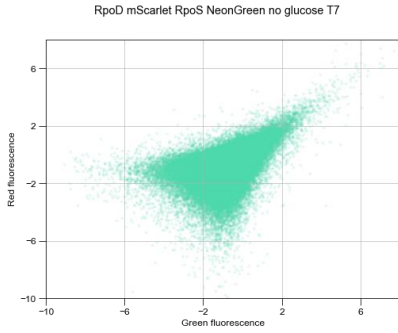
Analysing the calculated average, it is possible to see that both fluorescent signals show an increasing trend (Figure 19A), with no distinction between growth phases (Figure 19B). This means that both housekeeping and stress response sigma factors are being expressed at an increasing trend. Although both signals are increasing, the relative increase is greater for the green one, therefore, for the sigma factor  $\sigma^S$  expression.

Between the last two measurements, more than 15 hours of cell culture have passed, and it is possible to see that the expression of  $\sigma^D$  increased while the expression of  $\sigma^S$  decreased. Considering the twenty hours in total culturing the same cells, the environment from this culture must present at least some level of different stresses. Even then, the stress response sigma factor  $\sigma^S$  shows a decreasing trend.

### 4.3.3 Sigma factors expression in stress-inducing conditions

Flow cytometry experiments were performed in a stress-inducing environment to measure gene expression under these conditions and compare it with the previous experiment. To induce stress, cells were cultured in minimal medium with glucose and then transferred to the same medium without any carbon source. The construct fluorescence was acquired using the same settings (Figure 20).

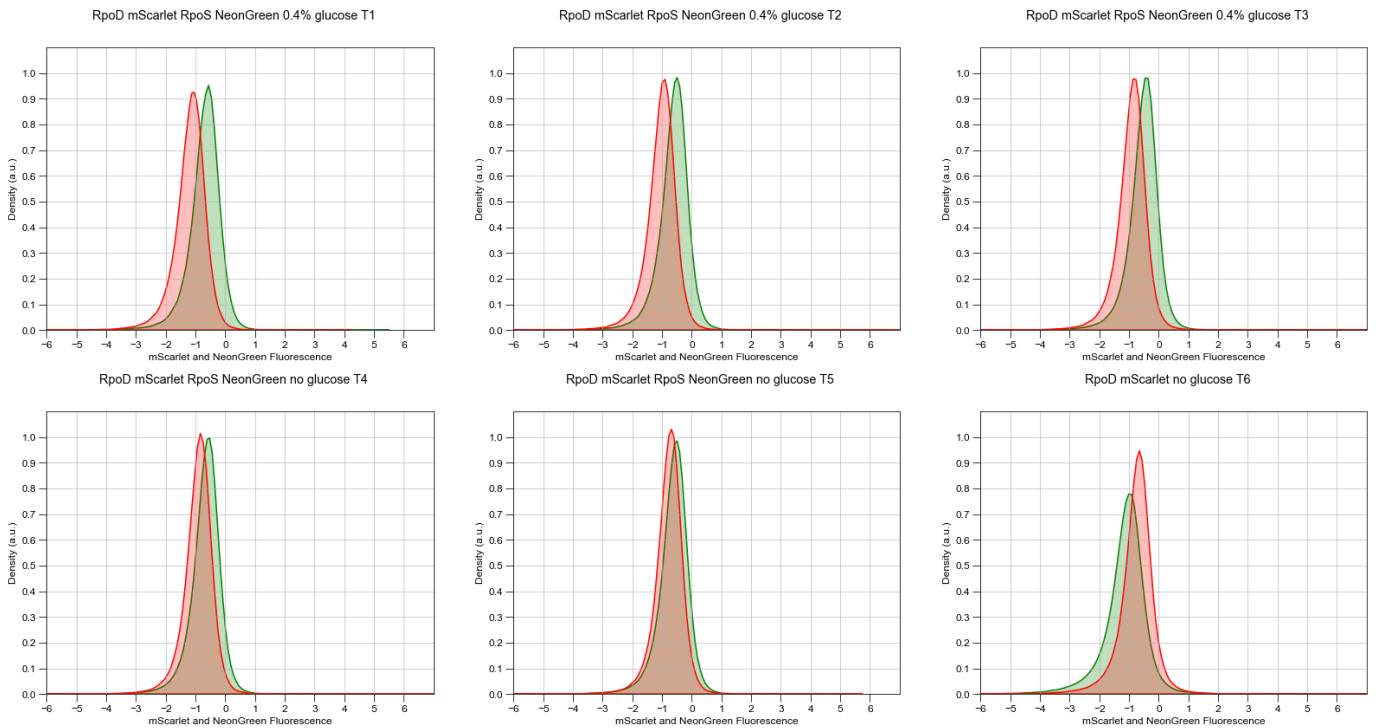




**Figure 20** - *E. coli* MG1655 generated strain containing the red reporter downstream  $\sigma^D$  and the green reporter downstream  $\sigma^S$  fluorescence signal acquired with flow cytometry during stress-inducing conditions. The first three time points were measured during growth in glucose and the next four time points were acquired in the absence of glucose.

The fluorescence data from the stress-inducing plots was corrected by the cell size by dividing the acquired fluorescence values by FSC-A (Forward scatter area) values. The culture was transferred to the medium without a carbon source after three measurements, so it is possible to see growth only in the first three scatter plots (Figure 20). After the nutrient privation, the fluorescence signal for both colours increased.

Density graphs were plotted from this same data (Figure 21).



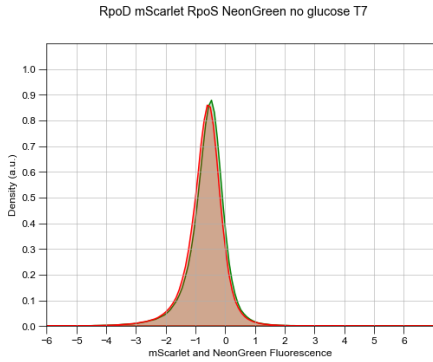


**Figure 21** - Sigma factors expression of *E. coli* MG1655 generated strain containing the red reporter downstream  $\sigma^D$  and the green reporter downstream  $\sigma^S$  in fluorescence density plots, acquired with flow cytometry during stress-inducing conditions

The first three time points were measured during growth in glucose and the next four time points were acquired in the absence of glucose.  $\sigma^D$  expression in red and  $\sigma^S$  expression in green.

In the first three time points, cells are growing in glucose and show a high green fluorescence (Figure 21), accordingly to previous results. After the fourth time point, cells were private from glucose and showed a higher red fluorescence until the last time point, in which both red and green signals are similar. Therefore, these results revealed that the expression of the housekeeping  $\sigma^D$  is increased under glucose deprivation.

The average fluorescence from the cell population was calculated for every time point in this case too (Figure 22).

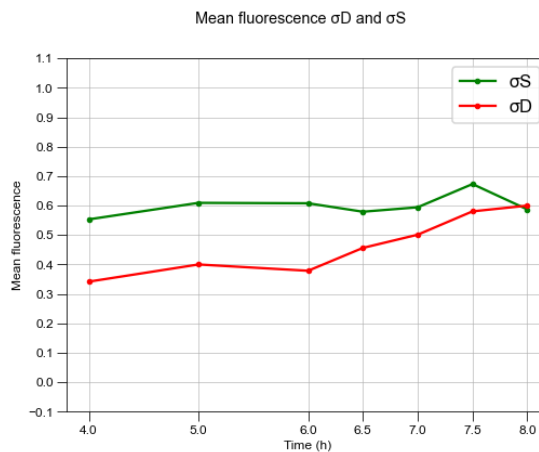


**Figure 22** – Average sigma factors expression of *E. coli* MG1655 constructed strain containing the red reporter downstream  $\sigma^D$  and the green reporter downstream  $\sigma^S$ , acquired with flow cytometry during stress-inducing conditions. The first three time points were measured during growth in glucose and the next four time points were acquired in the absence of glucose.

The average fluorescence from stress-inducing measurements (Figure 23) was corrected by discounting the fluorescence values of wild-type (Figure 18A) from the construct fluorescence values (Figure 22). The same values from previous experiments were considered for wild-type background adjusting.

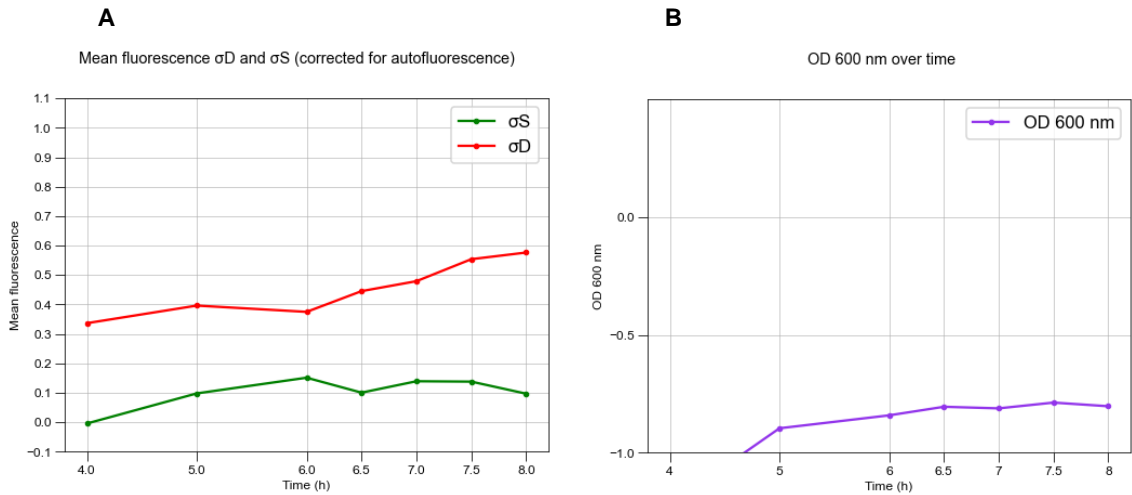


**Figure 23 – (A)** Average sigma factors expression of *E. coli* MG1655 constructed strain containing the red reporter downstream  $\sigma^D$  and the green reporter downstream  $\sigma^S$ , acquired with flow cytometry during stress-inducing conditions and corrected by wild-type autofluorescence. **(B)** Cell growth of the same strain acquired under stress-inducing conditions. The first three time points were measured during growth in glucose and the next four time points were acquired in the absence of glucose.

It is possible to see a change in the expression of both housekeeping and stress-response sigma factors after the moment of glucose deprivation. The red signal from  $\sigma^D$  expression shows an increasing trend after the third time point and the green signal from  $\sigma^S$  expression shows a decreasing trend (Figure 23A). In the OD graph, it is evident that cells stopped growing after being transferred to the medium without any carbon source (Figure 23B).

## 5. Discussion

Bacteria are constantly exposed to different stressful environments, experiencing temperature or pH variation or more general stresses, such as entry into stationary phase or nutrient depletion (Kim, 2020). Transcription initiation is a crucial point of gene expression regulation because of sigma factors competition for core-RNAP, a mechanism that allows the cells to adapt to changes in nutritional supply to grow rapidly in different environments. Persister cells can survive these and many environmental changes because of their high tolerance to antibiotics and other kinds of stresses, representing a wide health issue. The mechanism that triggers persistence remains unknown and since persisters are stress-tolerant and slow-growing variants of regular cells, the hypothesis was raised that the stress response sigma factor  $\sigma^S$  could be involved in persister cells formation.

In this context, this study focuses on understanding better the trade-off between the sigma factors and core RNA Polymerase by measuring gene expression of constitutive sigma factor  $\sigma^D$  and stress response sigma factor  $\sigma^S$  and learning whether  $\sigma^S$  plays a role in the persister cells formation by testing the hypothesis that under growth-favourable conditions, a tiny fraction of cells is already expressing more sigma  $\sigma^S$  than the housekeeping  $\sigma^D$ .

In order to achieve this, fluorescent reporters were correctly inserted in the *E. coli* genome downstream the sigma factors  $\sigma^D$  and  $\sigma^S$ , respectively, using the two plasmids CRISPR-Cas9 method (Jiang et al., 2015; Kang et al., 2022). The insertions were confirmed using PCR and DNA sequencing techniques. This method was preferred over tagging each sigma factor of interest with the reporters considering not to interfere with the sigma factors function. Also, inserting the reporters directly into the chromosome gives a little extra fluorescence than tagging the genes, considering the fluorescent reporters are very stable, and this facilitates the detection of fluorescence.

Two different strains were generated by the CRISPR-Cas9 system: one containing the red fluorescent protein right after the sigma factor  $\sigma^D$  and the other as well having the red fluorescent protein in the same position in the genome but also containing a green fluorescent protein after the sigma factor  $\sigma^S$ . Microscopy images of both generated strains were taken and compared to wild type in the red and green channels (Figure 10). The images showed the expression of the fluorescent reporters and confirmed it was possible to distinguish between the constructs and wild type. The construct containing the red reporter after  $\sigma^D$  showed fluorescence only in the red

channel, and the construct containing both red and green reporters after  $\sigma^D$  and  $\sigma^S$  showed fluorescence on both red and green channels. As expected, the wild type did not reveal any fluorescence on red or green channels. Although *E. coli* cells are known for having considerably high green autofluorescence (Mihalcescu et al., 2015; Galbusera et al., 2020), it was possible to distinguish between the construct and wild-type images.

From the growth experiments, it was possible to estimate the sigma factors' expression, at an average cell population level using the plate reader and at a single-cell level using flow cytometry. Fluorescence from wild-type cells was measured in all experiments, for comparison.

At an average cell population level, the expression of  $\sigma^D$  and  $\sigma^S$  revealed an increasing trend during growth, especially in the exponential phase. Both housekeeping and stress response sigma factors were expressed similarly during growth, which was not expected. Considering each one has a function of transcribing genes required in very different situations (growth and stress) and the fact that one inhibits the other, it was expected that expression would not occur at the same time.

The high green autofluorescence was a limitation of these experiments, making it difficult to visualize gene expression from the green reporter. Also making the two fluorescence signals too apart from each other in the plots, which were normalised by dividing the construct fluorescence values by wild-type measured fluorescence values. Even so, the construct fluorescence was easily distinguished from wild-type background fluorescence.

At a single-cell level, the flow-cytometry experiments revealed that both housekeeping and stress response sigma factors were expressed at an increasing trend during growth. The relative increase is greater for the sigma factor  $\sigma^S$  expression, but again the sigma factors show similar expression. Except for the last two measurements, which have more than 15 hours of culture between them: the  $\sigma^D$  shows an increased trend expression and the  $\sigma^S$  shows a decreased trend. After this 15-hour period, the cells were certain in the stationary phase of growth and the nutrients were depleted considering the volume of the culture (around 50 mL). In this case, the decreasing expression of the sigma responsible for stress response and the increased expression of the housekeeping sigma is, at least, unexpected.

The flow-cytometry experiments under stress induction conditions showed according results. The first three measurements were taken from a culture of cells containing glucose as a carbon source and showed constant expression of  $\sigma^D$  and an increasing trend in  $\sigma^S$  expression. After this, the same cells were washed and cultivated without any carbon source, using the same minimal medium except for the glucose. The

measurements from this culture showed an increasing trend in  $\sigma^D$  expression after the carbon source was taken from the cell culture and a decreasing trend in  $\sigma^S$  expression.

Regarding the hypothesis that under growth-favourable conditions, a small fraction of cells is already expressing more sigma  $\sigma^S$  than the housekeeping  $\sigma^D$ , from the flow-cytometry experiments it was not possible to observe any subpopulation of cells under either favourable or stress induction conditions. Further studies are necessary to clarify this hypothesis.

There were several technical difficulties involved in this study. First, it is generally difficult to measure a sigma factor expression, which is the reason there has been a gap period in studying sigma factors in the literature. A sigma factor is a very small molecule, which means it is hard to detect fluorescent reporters attached to it. In addition to this, it has an essential function in the metabolism of the cell, which means any reporter system could interfere on that function and report activities that are not a reflection of what actually happens, making the report system useless.

Another difficulty found was the high background green fluorescence in *E. coli* cells. Although measuring the green fluorescent signal at these expression levels worked well using microscopy, it was difficult to quantify the green fluorescence signal in the growth experiments, in both methods used (flow cytometry and plate reader). Mainly because it was difficult to distinguish between the green signal from the expression of  $\sigma^S$  than the autofluorescence of cells, but also because the red and green signals were too apart from each other. This led to making large corrections in the acquired data, normalizing the generated plots from these data, which can introduce errors. In other words, the acquired expression behaviour of both sigma factors is not established.

In addition to this, the regulation of alternative sigma factors is usually complex, with multiple tiers of control to regulate both their expression levels and activities (Österberg, 2011). The alternative sigma factors frequently are under tight negative regulation to avoid their competition for core-RNAP in conditions that they are not required (Battesti, 2011). More specifically, the regulation of  $\sigma^S$ , the sigma factor of interest in this study, involves transcription, mRNA turnover, translation initiation, and proteolysis (Brown et al., 2002). This study was aiming to measure the gene expression of this sigma factor (and also  $\sigma^D$ ), considering there is important regulation occurring at transcriptional levels. But perhaps this is a potential flaw in the design of experiments since the post-transcriptional regulation of RpoS can mislead our observation of gene expression. Nevertheless, there is considerable doubt whether all regulation happens at this level or if this is the most important level of regulation.



An important mediator of sigma factor competition and important regulation of transcription is the alarmone molecule (p)ppGpp. This molecule is the primary mediator of stringent response (Kvint, 2000; Österberg, 2011; Sharma, 2010) and plays a crucial role in the cellular capacity to adapt during survival responses (Nyström, 2004; Österberg, 2011). In this context, a point to consider is that according to Brown et al. (2002), the  $\sigma^S$  mRNA translation is increased by (p)ppGpp, not the transcription. It has been shown that ppGpp increases the rate of RpoS gene translation, and with the reporter system from this study, we are looking at transcription.

Another factor to consider is that during the stationary phase, the levels of  $\sigma^S$  go up to 30% of the  $\sigma^D$  levels (Sharma, 2010). So even when  $\sigma^S$  is required, its maximum level is less than half of  $\sigma^D$  levels. Considering that the green fluorescence background is high, it may be difficult to see an increase in the  $\sigma^S$  expression, because the absolute numbers are still quite low. Also, maybe this can explain why  $\sigma^D$  is expressed even in the stationary phase and or under stress conditions.

Even though the results are preliminary, as stated above, there are some consistent trends from the growth experiments, considering both approaches have accordingly results. The housekeeping and stress response sigma factors were expressed similarly during growth at average population cell level and single-cell level. These experiments revealed that both  $\sigma^D$  and  $\sigma^S$  were expressed at an increasing trend during growth, which can be explained by two reasons:

Firstly, according to Baptista et al. (2022), most *E. coli* genes that respond to both sigma  $\sigma^D$  and  $\sigma^S$  have their protein concentration increased when cells shift to stationary growth. Considering the design of the growth experiments, in which measures were taken during exponential phase every half an hour until cells reached to stationary phase, this can relate to why the studied sigma factors would be expressed with similar rates.

Secondly, the increasing trend in the expression of  $\sigma^S$  is likely induced by very low levels of exponential growth in order to elevate ppGpp levels (Brown et al., 2002). The increasing trend of  $\sigma^S$  was acquired in this study in the transition of cells from exponential to stationary growth. Once entered stationary phase, nutrients are depleted and stress levels start to increase, so the alarmone (p)ppGpp is required at this point to regulate the transition, which is coherent with this point.

In conclusion, the reporter system used in this study seems to work to some extent, since it is possible to see the gene expression of each sigma factor, but mostly using microscopy and not flow cytometry method. Additionally, the reporter system showed challenging issues that needed to be overcome, making it, perhaps, not the best approach to study sigma factors expression. Although the seen expression of each

sigma factor could be misled and post-transcriptional regulation was not considered, there was some consistency in the growth experiments at average population and single-cell level.

In this study, during the design of the experiments, it was chosen to insert the fluorescent reporters downstream *rpoD* and *rpoS* coding genes with a strong ribosome binding site considering this would give a stronger signal to detect, and, most important, it would not interfere with the function of each sigma factor inside the cell. However, lately, it was shown that it is possible, making it an interesting alternative approach to be used. Recently, Baptista et al. (2022) tagged the  $\sigma^S$  gene with the fluorescent protein mCherry (*rpoS::mCherry*) and they found a very low fluorescence signal until mid-exponential phase and after that, an increasing signal that was kept high at stationary phase. These results show that indeed there is some consistency in the acquired expression data from this study and also, show that this alternative approach is possible, without interfering with the sigma factors function.

## 6. Conclusions and future perspectives

In this work, it was possible to correctly insert fluorescent reporters into *E. coli* chromosome downstream the housekeeping  $\sigma^D$  and the stress response  $\sigma^S$  sigma factors. From growth experiments using the constructed strain, the average fluorescence showed an increasing trend for both sigma factors during growth. In addition, under stress conditions,  $\sigma^D$  fluorescence showed an increasing trend, but not  $\sigma^S$  fluorescence. It was not possible to see any subpopulation as hypothesised. Further studies are necessary to clarify this hypothesis.

For future work, the sigma factors can be tagged using fusion proteins. Using this approach, post-transcriptional regulations of  $\sigma^S$  would be considered. Furthermore, according to Baptista et al. (2022), only a tiny fraction of the promoters is responsive to both  $\sigma^D$  and  $\sigma^S$ . Therefore, another suggestion is to insert fluorescent reporters downstream the promoters that can recognise one or the other.

## 7. References

- Amato, S. M., Brynildsen, M. P. Nutrient Transitions Are a Source of Persisters in *Escherichia coli* Biofilms. *PLoS ONE* **2014**, 9 (3), e93110. <https://doi.org/10.1371/journal.pone.0093110>
- Baćun-Družina, V., Butorac, A., Mrvčić, J., Dragičević, T. L., Stehlik-Tomas, V. Bacterial Stationary-Phase Evolution. *Food Technol. Biotechnol.* **2011** 49 (1), 13–23. <https://doi.org/10.1128/ecosalplus.ESP-0004-2018>.
- Baptista, I. S. C., Kandavalli, V., Chauhan, V., Bahrudeen, M. N. M., Almeida, B. L. B., Palma, C. S. D., Dash, S., Ribeiro, A. S. Sequence-dependent model of genes with dual  $\sigma$  factor preference. *Biochimica et Biophysica Acta (BBA) - Gene Regulatory Mechanisms* **2022**, 1865 (3), 194812. <https://doi.org/10.1016/j.bbagrm.2022.194812>
- Battesti, A., Majdalani, N., Gottesman, S. The RpoS-mediated General Stress Response in *Escherichia coli*. *Annu Rev Microbiol* **2011**, 65 (1), 189-213.
- Bernardo, L., Johansson, L., Solera, D., Skärfstad, E., Shingler, V. The guanosine tetraphosphate (ppGpp) alarmone, DksA and promoter affinity for RNA polymerase in regulation of  $\sigma^{54}$ -dependent transcription. *Molecular Microbiology* **2006** 60 (3), 749-764. <https://doi.org/10.1111/j.1365-2958.2006.05129.x>
- Botman, D., de Groot D. H., Schmidt, P., Goedhart, J., Teusink, B. In vivo characterization of fluorescent proteins in budding yeast. *Sci Rep.* **2019**, 9 (1), 2234. <https://doi.org/10.1038/s41598-019-38913-z>
- Brown, L., Gentry, D., Elliott, T., Cashel, M. DksA Affects ppGpp Induction of RpoS at a Translational Level. *Journal Of Bacteriology* **2002**, 184 (6), 4455-4465. <https://doi.org/10.1128/JB.184.16.4455>
- Cavaliere, P., Brier, S., Filipenko, P., Sizun, C., Raynal, B., Bonneté, F., Levi-Acobas, F., Bellalou, J., England, P., Chamot-Rooke, J., Mayer, C., Norel, F. The stress sigma factor of RNA polymerase RpoS/ $\sigma^S$  is a solvent-exposed open molecule in solution. *Biochemical Journal* **2018**, 475 (1), 341-354. <http://dx.doi.org/10.1042/bcj20170768>

Chauhan, R., Ravi, J., Datta, P., Chen, t., Schnappinger, D., Bassler, K. E., Balázsi, G., Gennaro, M. L. Reconstruction and topological characterization of the sigma factor regulatory network of *Mycobacterium tuberculosis*. *Nature communications* **2016**, 7 (1), 11062. <http://dx.doi.org/10.1038/ncomms11062>

Cho, B., Kim, D., Knight, E. M., Zengler, K. Palsson, B. O. Genome-scale reconstruction of the sigma factor network in *Escherichia coli*: topology and functional states. *BMC Biology* **2014**, 12 (4). <http://dx.doi.org/10.1186/1741-7007-12-4>

Davis, M., Kesthely, C., Franklin, E., MacLellan, S. The essential activities of the bacterial sigma factor. *Can. J. Microbiol* **2017**, 63 (2), 89-99. <http://dx.doi.org/10.1139/cjm-2016-0576>

Farewell, A., Kvint, K., Nyström, T. Negative regulation by RpoS: a case of sigma factor competition. *Molecular Microbiology* **1998**, 29 (4), 1039-1051.

Farnelid, H., Bentzon-Tilia, M., Andersson, A., Bertilsson, S., Jost, G., Labrenz, M., Jurgens, K., Riemann, L. Active nitrogen-fixing heterotrophic bacteria at and below the chemocline of the central Baltic Sea. *The ISME Journal* **2013**, 7 (7), 1413-1423. <http://dx.doi.org/10.1038/ismej.2013.26>

Feklístov, A., Sharon, B., Darst, S., Gross, C. Bacterial Sigma Factors: a historical, structural, and genomic perspective. *Annual Review Of Microbiology* **2014**, 68 (1), 357-376. <http://dx.doi.org/10.1146/annurev-micro-092412-155737>.

Fisher, R. A., Gollan, B., Helaine, S. Persistent bacterial infections and persister cells. *Nature Reviews Microbiology* **2017**, 15 (8), 453-464. <http://dx.doi.org/10.1038/nrmicro.2017.42>

Galbusera, L., Bellement-Theroué, G., Urchueguia, A., Julou, T., Nimwegen, E. Using fluorescence flow cytometry data for single-cell gene expression analysis in bacteria. *PLoS ONE* **2020**, 15 (10), e0240233. <https://doi.org/10.1371/journal.pone.0240233>

Gopalkrishnan, S., Nicoloff, H., Ades, S. E. Co-ordinated regulation of the extracytoplasmic stress factor, sigmaE, with other *Escherichia coli* sigma factors by

(p)ppGpp and DksA may be achieved by specific regulation of individual holoenzymes. *Mol Microbiol.* **2014**, 93 (3), 479-493. <http://dx.doi.org/10.1111/mmi.12674>

Gulitz, A., Stadie, J., Wenning, M., Ehrmann, M. A., Vogel, R. F. The microbial diversity of water kefir. *International Journal of Food Microbiology* **2011**, 151 (3), 284-288. <http://dx.doi.org/10.1016/j.ijfoodmicro.2011.09.016>

Haldenwang, W. G. The sigma factors of *Bacillus subtilis*. *Microbiological Reviews* **1995**, 59 (1), 1-30.

Haurlyuk, V., Atkinson, G.C., Murakami, K. S., Tenson, T., Gerdes, K. Recent functional insights into the role of (p)ppGpp in bacterial physiology. *Nature Reviews Microbiology* **2015**, 13 (5), 298-309. <http://dx.doi.org/10.1038/nrmicro3448>

Jiang, Y., Chen, B., Duan, C., Sun, B., Yang, J., Yang, S. Multigene Editing in the *Escherichia coli* Genome via the CRISPR-Cas9 System. *Applied and Environmental Microbiology* **2015**, 81 (7), 2506-2514. <https://doi.org/10.1128/AEM.04023-14>

Jishage, M., Kvint, K., Shingler, V., Nyström, T. Regulation of  $\sigma$  factor competition by the alarmone ppGpp. *Genes & Development* **2002**, 16 (10), 1260-1270. <http://dx.doi.org/10.1101/gad.227902>

Kaldalu, N., Haurlyuk, V., Turnbull, K. J. Mensa, A. L., Putrinš, M. Tenson, T. *In Vitro* Studies of Persister Cells. *Microbiology and Molecular Biology Reviews* **2020**, 84 (4), e00070-20. <https://doi.org/10.1128/MMBR.00070-20>.

Kandavalli, V. K., Tran, H., Ribeiro, A. S. Effects of  $\sigma$  factor competition are promoter initiation kinetics dependent. *Biochimica et Biophysica Acta* **2016**, 1859 (10), 1281-1288. <http://dx.doi.org/10.1016/j.bbagr.2016.07.011>

Kang, X., Zhou, X., Tang, Y., Jiang, Z., Chen, J., Mohsin, M., Yue, M. Characterization of Two-Component System CitB Family in *Salmonella Pullorum*. *Int. J. Mol. Sci.* **2022**, 23 (17), 10201. <https://doi.org/10.3390/ijms231710201>

Kim, W., Lee, Y. Mechanism for coordinate regulation of *rpoS* by sRNA-sRNA interaction in *Escherichia coli*. *RNA Biology* **2020**, 17 (2), 176-187. <https://doi.org/10.1080/15476286.2019.1672514>

Kvint, K., Farewell, A., Nyström, T. RpoS-dependent Promoters Require Guanosine Tetraphosphate for Induction Even in the Presence of High Levels of  $\sigma^s$ . *The Journal of Biological Chemistry* **2000**, 275 (20), 14795-14798. <http://dx.doi.org/10.1074/jbc.C000128200>

Lewis, K. Persister Cells. *Annual Review Of Microbiology* **2010**, 64 (1), 357-372. <http://dx.doi.org/10.1146/annurev.micro.112408.134306>

Li, L., Fang, C., Zhuang, N., Wang, T. Zhang, Y. Structural basis for transcription initiation by bacterial ECF  $\sigma$  factors. *Nature communications* **2019**, 10 (1), 1153. <http://dx.doi.org/10.1038/s41467-019-09096-y>

Liu, J. M., Xin, X. J., Li, C. X., Xu, J. H., Bao, J. Cloning of thermostable cellulase genes of *Clostridium thermocellum* and their secretive expression in *Bacillus subtilis*. *Applied biochemistry and biotechnology* **2012**, 166 (3), 652-662. <http://dx.doi.org/10.1007/s12010-011-9456-z>

Magnusson, L. U., Farewell, A., Nyström, T. ppGpp: a global regulator in *Escherichia coli*. *Trends in Microbiology* **2005**, 13 (5), 236-242. <http://dx.doi.org/10.1016/j.tim.2005.03.008>

Mihalcescu, I., Van-Melle Gateau, M. Chelli, B., Pinel, C., Ravanat, J. Green autofluorescence, a double edged monitoring tool for bacterial growth and activity in micro-plates. *Phys. Biol.* **2015**, 12 (6), 066016. <http://dx.doi.org/10.1088/1478-3975/12/6/066016>

Miyae, S., Suzuki, E., Komiyama, Y., Kondo, Y., Morikawa, M., Maeda, S. Bacterial Memory of Persisters: Bacterial Persister Cells Can Retain Their Phenotype for Days or Weeks After Withdrawal From Colony–Biofilm Culture. *Frontiers in Microbiology* **2018**, 9 (1), 1396. <http://dx.doi.org/10.3389/fmicb.2018.01396>

Nandy, P. The role of sigma factor competition in bacterial adaptation under prolonged starvation. *Microbiology* **2022**, 168 (5), 001195. <http://dx.doi.org/10.1099/mic.0.001195>

Nyström, T. Growth versus maintenance: a trade-off dictated by RNA polymerase availability and sigma factor competition? *Molecular Microbiology* **2004**, 54 (4), 855–862. <http://dx.doi.org/10.1111/j.1365-2958.2004.04342.x>

Oguyenko, A., Petushkov, I., Pupov, D., Esyunina, D., Kulbachinskiy, A. Universal functions of the  $\sigma$  finger in alternative  $\sigma$  factors during transcription initiation by bacterial RNA polymerase. *RNA Biology* **2021**, 18 (11), 2028-2037. <https://doi.org/10.1080/15476286.2021.1889254>

Österberg, S., Peso-Santos, T., Shingler, V. Regulation of Alternative Sigma Factor Use. *Annual Review Of Microbiology* **2011**, 65 (1), 37-55. <http://dx.doi.org/10.1146/annurev.micro.112408.134219>

Pavlov, M. Y., Ehrenberg, M. Optimal control of gene expression for fast proteome adaptation to environmental change. *PNAS* **2013**, 110 (51), 20527-20532. <http://dx.doi.org/10.1073/pnas.130935611>

Piper, S. E., Mitchell, J. E., Lee, D. J., Busby, S. J. W. A global view of *Escherichia coli* Rsd protein and its interactions. *Molecular BioSystems* **2009**, 12 (5), 1943-1947. <http://dx.doi.org/10.1039/b904955j>

Potrykus, K., Cashel, M. (p)ppGpp: Still magical? *Annual Review Of Microbiology* **2008**, 62 (1), 35-51. <http://dx.doi.org/10.1146/annurev.micro.62.081307.162903>

Radzikowski, J. L., Vedelaar, S., Siegel, D., Ortega, A. D., Schmidt, A., Heinemann, M. Bacterial persistence is an active  $\sigma^S$  stress response to metabolic flux limitation. *Molecular Systems Biology* **2016**, 12 (9), 882. <http://dx.doi.org/10.15252/msb.20166998>

Roberts, J. W. Promoter-specific control of *E. coli* RNA polymerase by ppGpp and a general transcription factor. *Genes & Development* **2009**, 23 (2), 143-146. <http://dx.doi.org/10.1101/gad.1770509>



Sharma, U. K., Chatterji, D. Transcriptional switching in *Escherichia coli* during stress and starvation by modulation of  $\sigma^{70}$  activity. *Fems Microbiology Reviews* **2010**, 34 (5), 646-657. <http://dx.doi.org/10.1111/j.1574-6976.2010.00223.x>

Shimada, T., Furuhashi, S., Ishihama, A. Whole set of constitutive promoters for RpoN sigma factor and the regulatory role of its enhancer protein NtrC in *Escherichia coli* K-12. *Microbial Genomics* **2021**, 7 (11), 000653. <http://dx.doi.org/10.1099/mgen.0.000653>

Sutherland, C., Murakami, K. S. An Introduction to the Structure and Function of the catalytic core enzyme of *Escherichia coli* RNA polymerase. *EcoSal Plus* **2018**, 8 (1), 1-14. <http://dx.doi.org/10.1128/ecosalplus.ESP-0004-2018>

Zhao, S., Zhang, K., Jiang, S., Liu, Z., Wang, Z., Wang, Y., Liu, B. Resonance assignments of sigma factor S binding protein Crl from *Escherichia coli*. *Biomolecular NMR Assignments* **2019**, 13 (1), 223-226. <https://doi.org/10.1007/s12104-019-09881-2>

## 8. Supplementary material

**Supplementary Table 1** - List of primers used in this study

<b>Primer</b>	<b>Sequence</b>
pTarget_Fw	CAGCGAGTCAGTGAGCGAGGAA
pTarget_Rv	GCACTGTTGCAAATAGTCGGTGGT
pTarget_Fw2	GCCGCTCGCCAGTCGATT
pTarget_Rv2	AATCGACTGGCGAGCGGC
Fw_pTarget_N20rpoD_OH	GGCCTACCGATTAATCGTCCGTTTTAGAGCTAGAAATAGCAAGTTAA AATAAGGCTAGTCC
Rv_pTarget_N20rpoD_OH	GGACGATTAATCGGTAGGCCACTAGTATTATACCTAGGACTGAGCT AGCTGTC
Fw_N20rpoD_control	GACAGCTAGCTCAGTCCTAGGTATAATACTAGTGGCCTACCGATTA ATCGTCC
Fw_rpoD_sgRNA_OH	GACAGCTAGCTCAGTCCTAGGTATAATACTAGTGGCCTACCGATTA ATCGTCC
Rv_rpoD_sgRNA_OH	GGCGTTTCCATGGAGATTGGCTCCAAAAAAGCACCCGACTCGGTGC
Rv_rpoD_pamchange	TCTAAATTAATCGTCCAGAAAGCTACGCAGCACTTCAGAACG
Fw_mScarletl_pgk_OH	TTTAGAATCAACGAGAGGATTCACCATGGTGAGCAAGGGCGAG
Rv_rpoD_pgk_OH	GGTGAATCCTCTCGTTGATTCTAAATTAATCGTCCAGAAAGCTACGC AGC
Rv_mScarletl	CGGTGGACGCTTCCCAGC
Fw_dwnrpoD_mScarletl_OH	CGGCATGGACGAGCTGTACAAGTAATCGGTAGGCCGGATCAGGC
Rv_mScarletl_dwnrpoD_OH	GCCTGATCCGGCCTACCGATTACTTGTACAGCTCGTCCATGCCG
Fw_pTarget_DwnrpoD_OH	CCAACGCCTGCGGCTGATAATCCTCTAGAGTCGACCTGCAGAAGCT
Rv_DwnrpoD_Target_OH	AGCTTCTGCAGGTCGACTCTAGAGGATTATCAGCCGAGGCGTTGG
Fw_Up_rpoD	AAGAGATGGGCCGTGAACCGA
Rv_Dwn_rpoD	GGCGTCACCAAACCTGGTAGACC
Fw_pTarget_N20rpoS_OH	GACAGATGCTTACTTACTCGGTTTTAGAGCTAGAAATAGCAAGTTAA AATAAGGCTAGTCC
Rv_Target_N20rpos_OH	CGAGTAAGTAAGCATCTGTCACTAGTATTATACCTAGGACTGAGCTA GCTGTCA
Fw_sgRNA	GTTTTAGAGCTAGAAATAGCAAGTTAAAATAAGGCTAGTCC
Rv_sgRNA	CAAAAAAAGCACCCGACTCGGTGCC
Fw_rpoS_sgRNA_OH	GCACCGAGTCGGTGCTTTTTTTGGAGCGTTGCTGGACATCCTGG
Rv_rpoS_pgkRBS_OH	GGTGAATCCTCTCGTTGATTCTAAATTAATCGCGAAACAGCGCTTCG
Fw_neongreen_pgkRBS_OH	TTTAGAATCAACGAGAGGATTCACCATGGTGAGCAAGGGCGAGGA
Rv_neongreen_control	ACTGCATTGTGCGATGGACTTGG
Fw_DwnRpoS	TAAGTAAGCATCTGTACAGAAAGGCCAGTCT
Rv_neongreen_DwnRpoS_OH	CCTTTCTGACAGATGCTTACTTACTTGTACAGCTCGTCCATGCC

Fw_pTarget_DwnRpoS_OH	GACCCCTGCGCTCTAGAGTCGACCTGCAGAAGCT
Rv_DwnRpoS_pTarget_OH	TTCTGCAGGTGCGACTCTAGAGCGCAGGGGTCAGCAACCG
Fw_Up_rpoS	CGGAAGAGATCGCAGAGCAACTG
Rv_DwnRpoS	AATCGGGCGTCGGCAAAGC

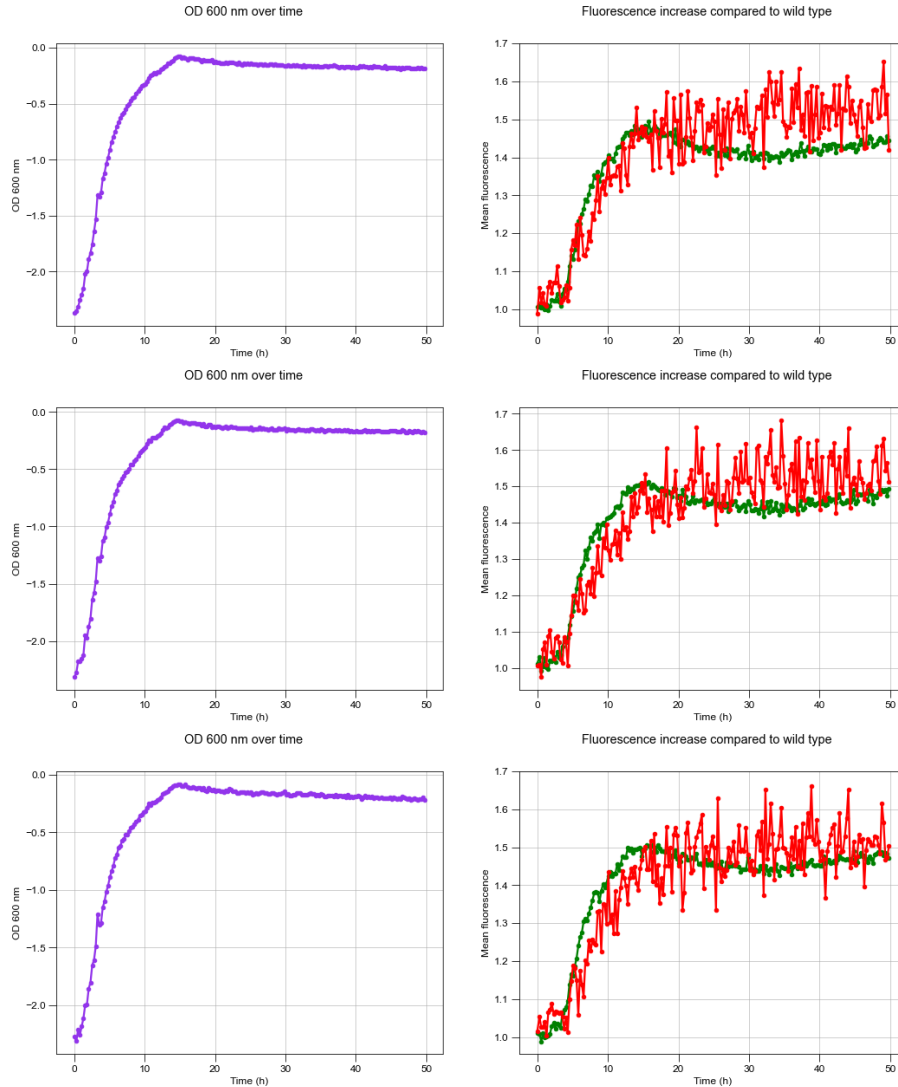
**Supplementary Table 2** - Clone 4 DNA sequencing after the reporter insertion

Sigma factor	Sequence
<b><math>\sigma^D</math> mScarlet1</b>	GAAGGCTGAACGTATGCTGATGCCGGAAGACAAGATCCGCAAAGTGCTGAAGATC GCCAAAGAGCCAATCTCCATGGAAACGCCGATCGGTGATGATGAAGATTCGCATC TGGGGGATTTTCATCGAGGATACCACCCTCGAGCTGCCGCTGGATTCTGCGACCAC CGAAAGCCTGCGTGCGGCAACGCACGACGTGCTGGCTGGCCTGACCGCGCGTG AAGCAAAAAGTTCTGCGTATGCGTTTTCGGTATCGATATGAACACCGACTACACGCTG GAAGAAGTGGGTAAACAGTTTCGACGTTACCCGCGAACGTATCCGTGATCGAAG CGAAGGCGCTGCGCAAAGTGCCTCACCCGAGCCGTTCTGAAGTGTGCGTAGCT TTCTGGACGATTAATTTAGAATCAACGAGAGGATTCACCATGGTGAGCAAGGGCG AGGCAGTGATCAAGGAGTTCATGCGGTTCAAGGTGCACATGGAGGGCTCCATGAA CGGCCACGAGTTCGAGATCGAGGGCGAGGGCGAGGGCCGCCCTACGAGGGCA CCCAGACCGCCAAGCTGAAGGTGACCAAGGGTGGCCCCCTGCCCTTCTCCTGGG ACATCCTGTCCCCTCAGTTCATGTACGGCTCCAGGGCCTTCATCAAGCACCCCGC CGACATCCCCGACTACTATAAGCAGTCCTTCCCCGAGGGCTTCAAGTGGGAGCGC GTGATGAACTTCGAGGACGGCGGCGCCGTGACCGTGACCCAGGACACCTCCCTG GAGGACGGCACCCCTGATCTACAAGGTGAAGCTCCGCGGCACCAACTTCCCTCCT GACGGCCCCGTAATGCAGAAGAAGACAATGGGCTGGGAAGCGTCCACCGAGCGG TTGTACCCCGAGGACGGCGTGTGAAGGGCGACATTAAGATGGCCCTGCGCCTG AAGGACGGCGGCCGCTACCTGGCGGACTTCAAGACCACCTACAAGGCCAAGAAG CCCGTGCAGATGCCCGGCGCCTACAACGTCGACCGCAAGTTGGACATCACCTCC CACAACGAGGACTACACCGTGGTGAACAGTACGAACGCTCCGAGGGCCGCCAC TCCACCGGCGGCATGGACGAGCTGTACAAGTAATCGGTAGGCCGGATCAGGCGT TACGCCGCACCCGGCACTAGGCCCTCTGCACAAACGCCACCTTTTCGGTGGCGTT TTTTATCGCCACGCAC

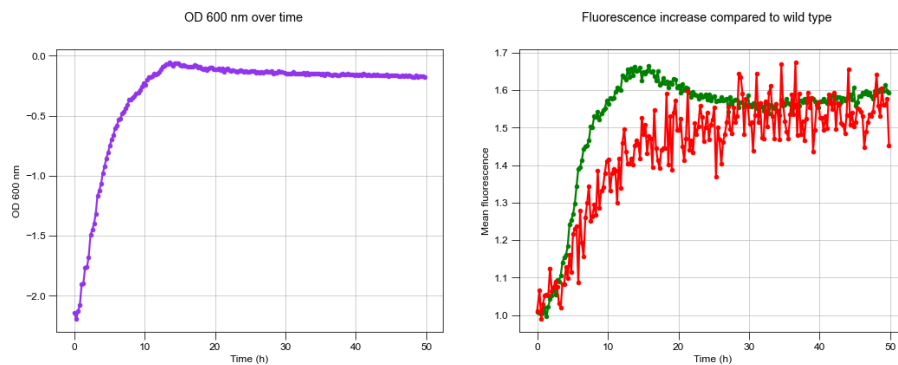
**Supplementary Table 3** - Clone 10 DNA sequencing after the reporters' insertion

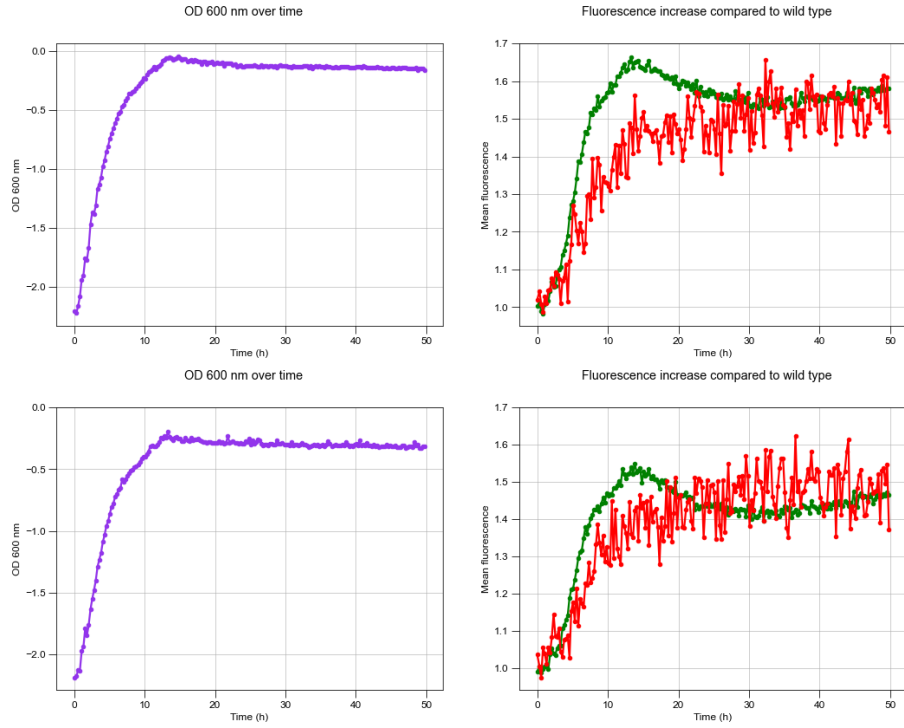
Sigma factor	Sequence
<p><math>\sigma^D</math> mScarlet1</p>	<p>GCTGAACGTATGCTGATGCCGGAAGACAAGATCCGCAAAGTGCTGAAGATCGCCAA  AGAGCCAATCTCCATGGAAACGCCGATCGGTGATGATGAAGATTGCGATCTGGGGG  ATTTTCATCGAGGATACCACCCTCGAGCTGCCGCTGGATTCTGCGACCACCGAAAGC  CTGCGTGCGGCAACGCACGACGTGCTGGCTGGCCTGACCGCGCGTGAAGCAAAAG  TTCTGCGTATGCGTTTCGGTATCGATATGAACACCGACTACACGCTGGAAGAAGTG  GGTAAACAGTTCGACGTTACCCGCGAACGTATCCGTGAGATCGAAGCGAAGGCGCT  GCGCAAACCTGCGTCACCCGAGCCGTTCTGAAGTGCTGCGTAGCTTTCTGGACGATT  AATTTAGAATCAACGAGAGGATTACCATGGTGAGCAAGGGCGAGGCAGTGATCAA  GGAGTTCATGCGTTCAAGGTGCACATGGAGGGCTCCATGAACGGCCACGAGTTC  GAGATCGAGGGCGAGGGCGAGGGCCGCCCTACGAGGGCACCCAGACCCGCCAAG  CTGAAGGTGACCAAGGGTGGCCCCCTGCCCTTCTCCTGGGACATCCTGTCCCCTCA  GTTTCATGTACGGCTCCAGGGCCTTCATCAAGCACCCCGCCGACATCCCCGACTACT  ATAAGCAGTCCTTCCCCGAGGGCTTCAAGTGAGGAGCGCGTGATGAACTTCGAGGAC  GGCGGCGCCGTGACCGTGACCCAGGACACCTCCCTGGAGGACGGCACCCCTGATCT  ACAAGGTGAAGCTCCGCGGCACCAACTTCCCTCCTGACGGCCCCGTAATGCAGAA  GAAGACAATGGGCTGGGAAGCGTCCACCGAGCGGTTGTACCCCGAGGACGGCGTG  CTGAAGGGCGACATTAAGATGGCCCTGCGCCTGAAGGACGGCGGCCGCTACCTGG  CGGACTTCAAGACCACCTACAAGGCCAAGAAGCCCGTGACAGATGCCCGGCGCCTA  CAACGTGACCCGCAAGTTGGACATCACCTCCCACAACGAGGACAACACC</p>
<p><math>\sigma^S</math> NeonGreen</p>	<p>GATGACGTCAGCCGTATGCTTTCGTTAACGAGCGCATTACCTCGGTAGACACCCC  GCTGGGTGGTGATTCCGAAAAAGCGTTGCTGGACATCCTGGCCGATGAAAAAGAGA  ACGGTCCGGAAGATAACCACGCAAGATGACGATATGAAGCAGAGCATCGTCAAATGG  CTGTTTCGAGCTGAACGCCAAACAGCGTGAAGTGCTGGCACGTCGATTCCGTTTGCT  GGGGTACGAAGCGGCAACACTGGAAGATGTAGGTCGTGAAATTGGCCTCACCCGT  GAACGTGTTCCGAGATTGAGTTGAAGGCCTGCGCCGTTTGCGCGAAATCCTGCA  AACGCAGGGGCTGAATATCGAAGCGCTGTTTCGCGAGTAATTTAGAATCAACGAGA  GGATTCACCATGGTGAGCAAGGGCGAGGAGGATAACATGGCCTCTCTCCCAGCGA  CACATGAGTTACACATCTTTGGCTCCATCAACGGTGTGGACTTTGACATGGTGGGTC  AGGGCACCCGGCAATCCAAATGATGGTTATGAGGAGTTAAACCTGAAGTCCACCAAG  GGTGACCTCCAGTTCTCCCCCTGGATTCTGGTCCCTCATATCGGGTATGGCTTCCAT  CAGTACCTGCCCTACCCTGACGGGATGTCGCCTTTCAGGCCGCCATGGTAGATGG  CTCCGGCTACCAAGTCCATCGCACAAATGCAGTTTGAAGATGGTGCCTCCCTTACTGT  TAACTACCGCTACACCTACGAGGGAAGCCACATCAAAGGAGAGGCCAGGTGAAG  GGGACTGGTTTCCCTGCTGACGGTCTGTGATGACCAACTCGCTGACCGCTGCGGA  CTGGTGCAGGTCAAGAAGACTTACCCCAACGACAAAACCATCATCAGTACCTTTAA  GTGGAGTTACCACTGGAATGGCAAGCGCTACCGGAGCACTGCGCGGACCACC  TACACCTTTGCCAAGCCAATGGCGGCTAACTATCTGAAGAACCAGCCGATGTACGT  GTTCCGTAAGACGGAACCTCAAGCACTCCAAGAACGAGCTCAACTTCAAGGAGTG</p>

**Supplementary Figure 1** – *E. coli* MG1655 generated strain containing the single red reporter on  $\sigma^D$  cell growth and sigma factors expression from plate reader experiment  
 OD<sub>600 nm</sub> measured over time (left) and acquired fluorescence signal from the constructed strain compared to wild-type,  $\sigma^D$  expression in red and green autofluorescence from *E. coli* (right).

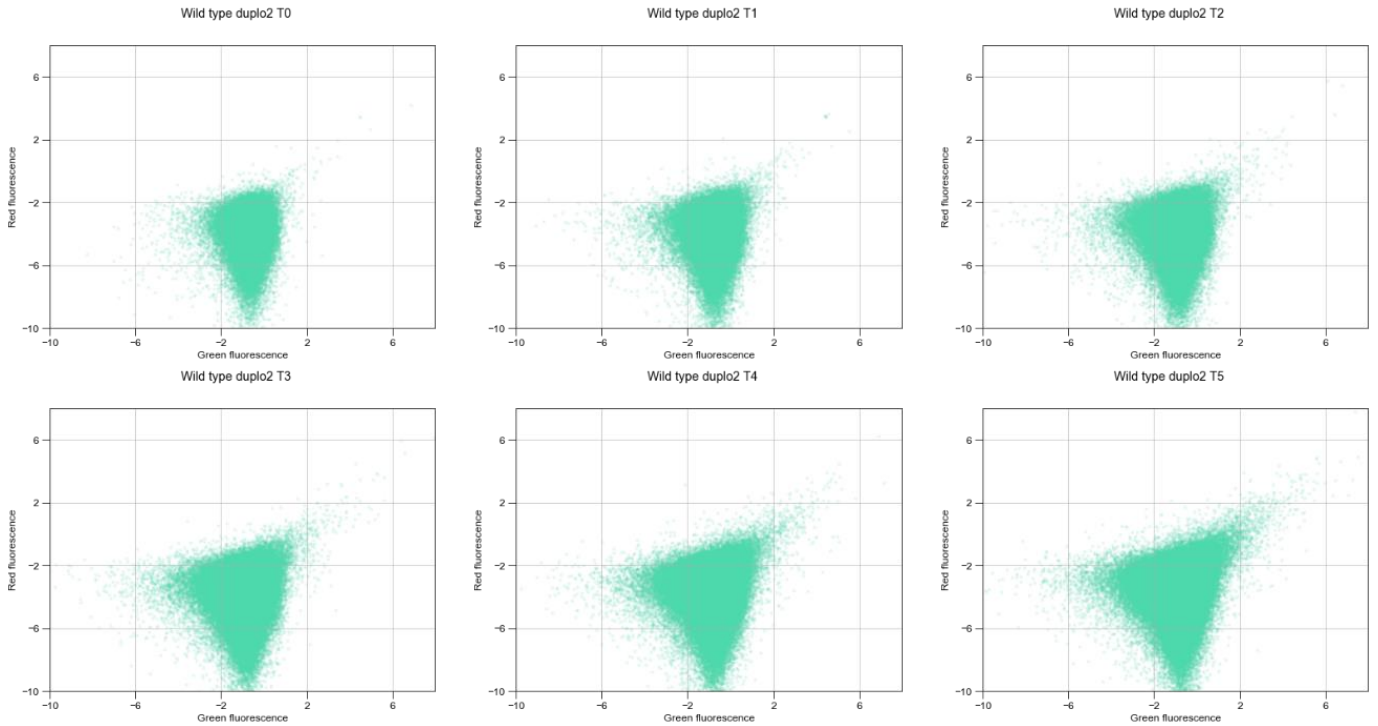


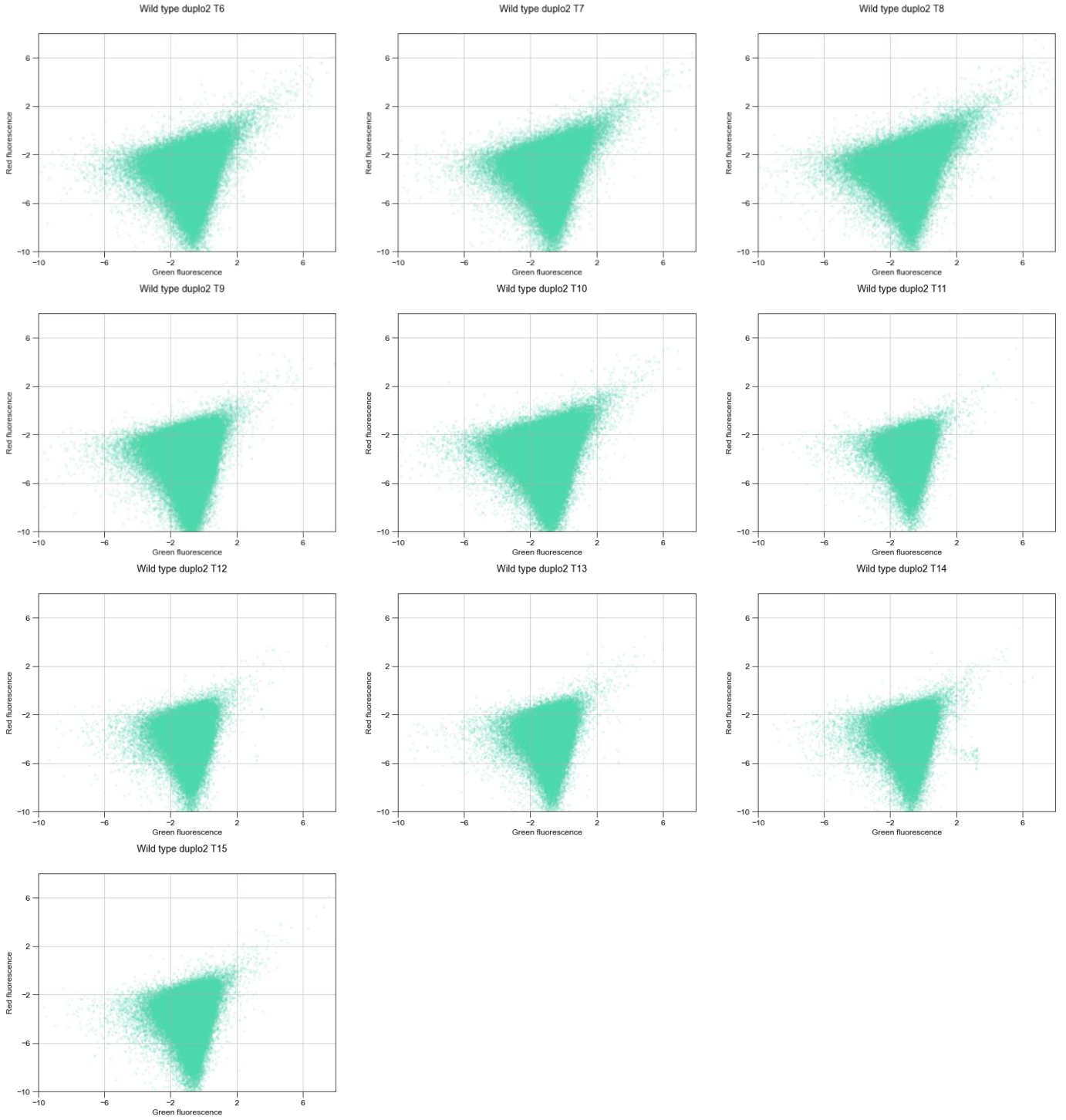
**Supplementary Figure 2** – *E. coli* MG1655 generated strain containing both red and green reporters on  $\sigma^D$  and  $\sigma^S$  cell growth and sigma factors expression from plate reader experiment  
 OD<sub>600 nm</sub> measured over time (left) and acquired fluorescence signal from the constructed strain compared to wild-type,  $\sigma^D$  expression in red and  $\sigma^S$  expression in green (right).



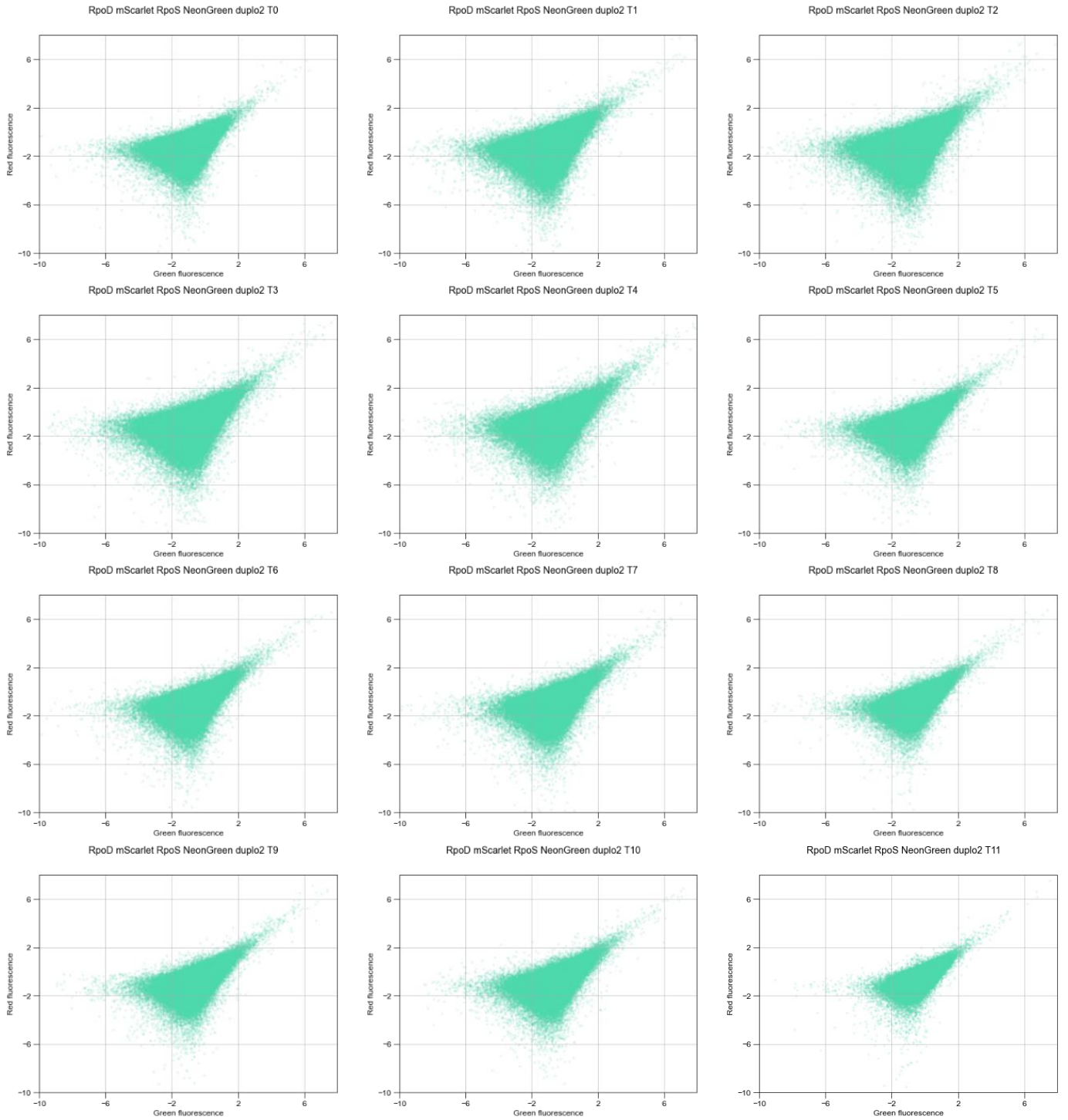


**Supplementary Figure 3** - *E. coli* MG1655 autofluorescence acquired with flow cytometry, used as control. Measurements acquired every thirty minutes from early exponential phase culture.

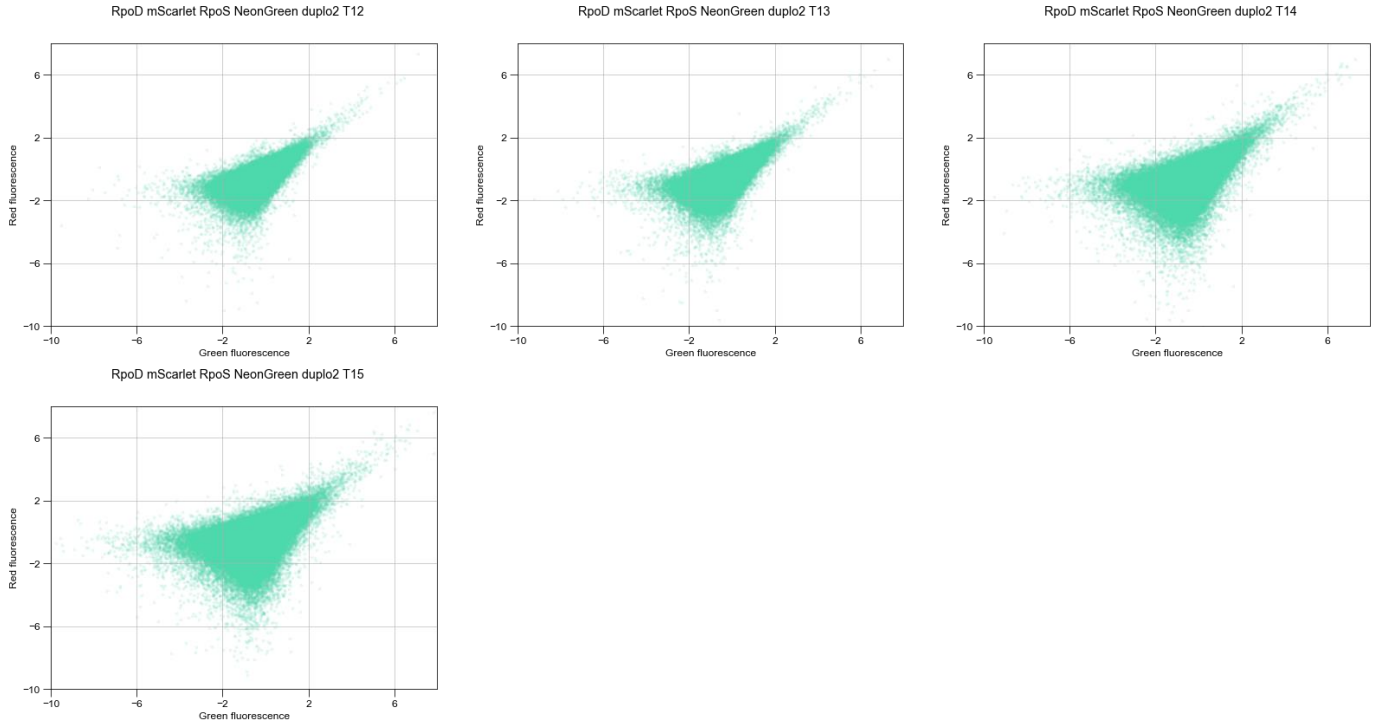




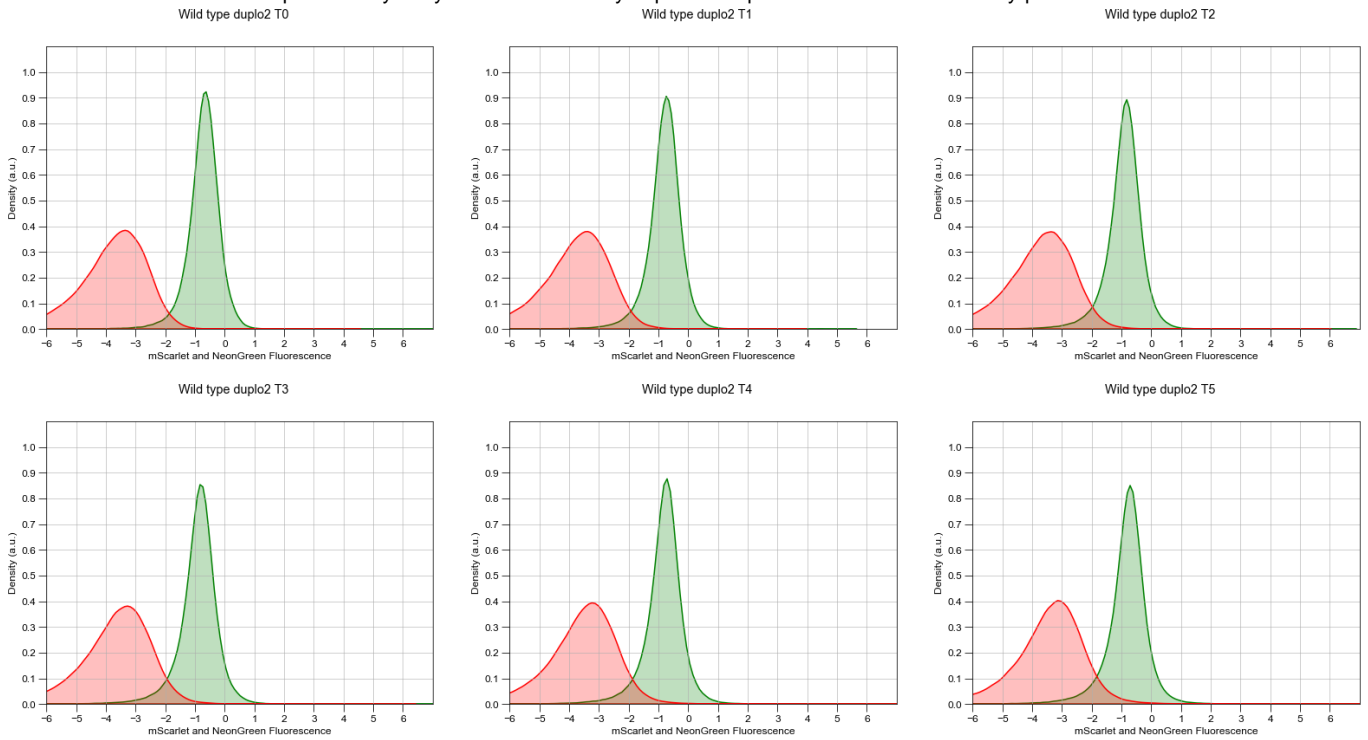
**Supplementary Figure 4** - *E. coli* MG1655 generated strain containing the red reporter downstream  $\sigma^D$  and the green reporter downstream  $\sigma^S$  fluorescence signal acquired with flow cytometry. Measurements acquired every thirty minutes from early exponential phase culture until stationary phase





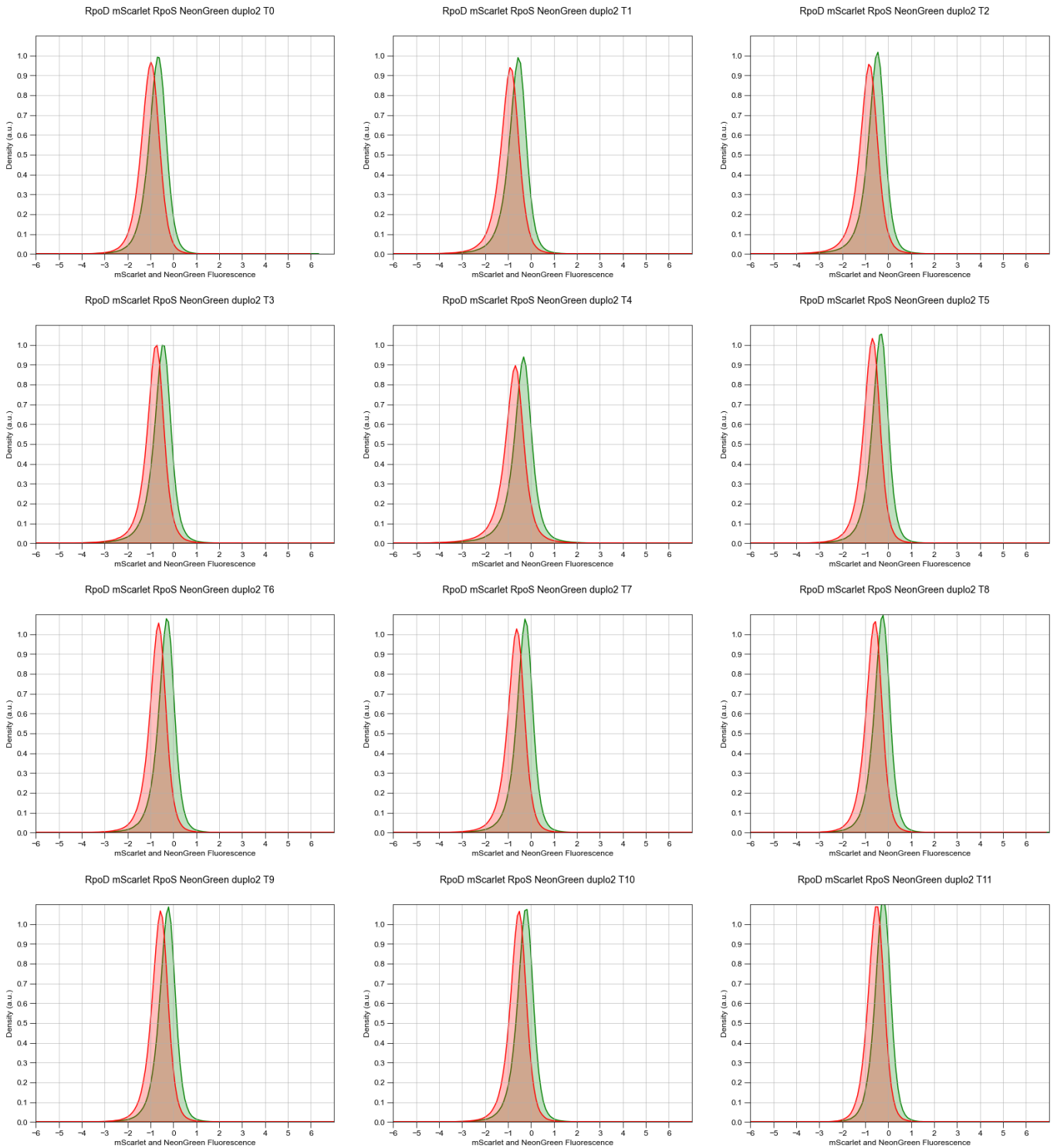


**Supplementary Figure 5 - *E. coli* MG1655 autofluorescence density plots, acquired with flow cytometry, used as control Measurements acquired every thirty minutes from early exponential phase culture until stationary phase.**

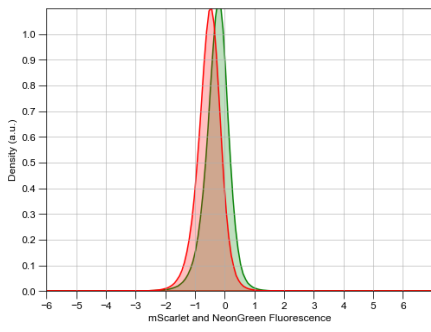




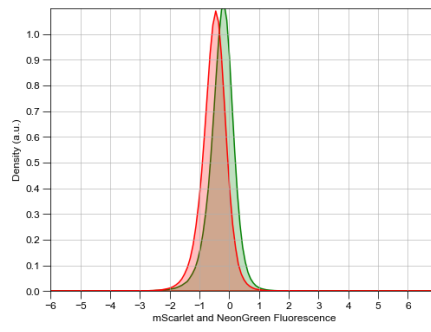
**Supplementary Figure 6** - Sigma factors expression of *E. coli* MG1655 generated strain containing the red reporter downstream  $\sigma^D$  and the green reporter downstream  $\sigma^S$  in fluorescence density plots, acquired with flow cytometry. Measurements acquired every thirty minutes from early exponential phase culture until stationary phase.  $\sigma^D$  expression in red and  $\sigma^S$  expression in green.



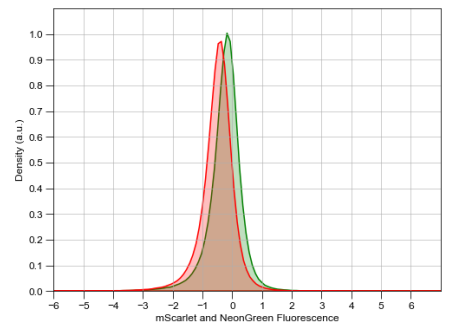
RpoD mScarlet RpoS NeonGreen duplo2 T12



RpoD mScarlet RpoS NeonGreen duplo2 T13



RpoD mScarlet RpoS NeonGreen duplo2 T14



RpoD mScarlet RpoS NeonGreen duplo2 T15

